

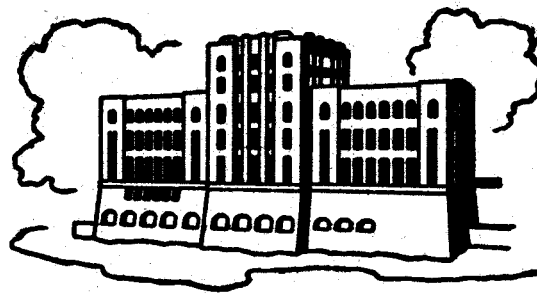
FILE COPY

TRANSVERSE MIXING CHARACTERISTICS OF THE MISSOURI RIVER DOWNSTREAM FROM THE COOPER NUCLEAR STATION

by
William W. Sayre
and
Tso-Ping Yeh

Prepared for
Nebraska Public Power District
Columbus, Nebraska

PLEASE DO NOT REMOVE



IIHR Report No. 145

**Iowa Institute of Hydraulic Research
The University of Iowa
Iowa City, Iowa**

April, 1973

**TRANSVERSE MIXING CHARACTERISTICS OF THE
MISSOURI RIVER DOWNSTREAM FROM
THE COOPER NUCLEAR STATION**

by
**William W. Sayre
and
Tso-Ping Yeh**

Prepared for
Nebraska Public Power District
Columbus, Nebraska

IIHR Report No. 145

Iowa Institute of Hydraulic Research
The University of Iowa
Iowa City, Iowa

April, 1973

ABSTRACT

The transverse mixing characteristics of the Missouri River in the vicinity of the Cooper Nuclear Station near Brownville, Nebraska, were investigated using the fluorescent-dye tracer technique. Rhodamine WT dye, introduced continuously into the plant once-through circulating-water system, was used to simulate the waste heat. Transverse profiles of dye concentration, depth, and velocity were obtained at several cross sections in the six-mile reach immediately downstream from the plant.

The results indicate that the excess temperature in the river at full plant load can be reduced by dilution to less than 5°F within a 45-acre mixing zone with the present discharge canal system, provided that the river discharge is not less than about 20,000 cfs. For lower river discharges, some additional mixing would be required to achieve the same reduction.

Based on a more detailed analysis of the transverse mixing process, the dimensionless transverse mixing coefficient in the six-mile reach downstream from the plant was found to have average and maximum values that are believed to considerably exceed any previously published values.

ACKNOWLEDGMENTS

This investigation was sponsored by the Nebraska Public Power District, Columbus, Nebraska, through the office of Dr. E.N. Sloth, Environmental Manager of NPPD. Participants in the investigation included personnel from the Iowa Institute of Hydraulic Research of The University of Iowa (IIHR); Industrial Bio-Test Laboratories, Inc., Northbrook, Illinois; Minnesota District of the U.S. Geological Survey (USGS); and the Nebraska Public Power District (NPPD). The USGS group from Minnesota which included T. Ross, J. Hess and D. Wicklund, obtained the channel depth and velocity distribution data by the moving boat method. The Bio-Test group which included M.P. Locke, S. Reetz, and others, collected and analyzed the dye samples. The system for introducing the dye tracer into the plant circulating-water system was set up and monitored by E.J. Miller and Y. Onishi (IIHR) with the assistance of W. Bell and T. Hendricks (NPPD). Members of the transit and spotting party included V. Wolstenholm and L. Schneider (NPPD) and E.J. Schiller and T.P. Yeh (IIHR). J. Cooper (NPPD) coordinated the preparations for the experiment at the plant site. Overall supervision and coordination was provided by W.W. Sayre (IIHR) who, together with T.P. Yeh, analyzed the data and prepared this report.

TABLE OF CONTENTS

	Page No.
ABSTRACT	i
ACKNOWLEDGMENTS	ii
LIST OF TABLES	iv
LIST OF FIGURES	iv-v
LIST OF SYMBOLS	vi-vii
I. BACKGROUND	1
II. DESCRIPTION OF TEST REACH	3
III. DESCRIPTION OF EXPERIMENT	5
A. Dye Introduction	5
B. Sample Collection	13
C. Analysis of Samples	13
IV. PRESENTATION OF RESULTS	14
A. Dye Distribution in the Discharge Canal	14
B. Transverse Distribution of Dye Concentration	14
C. Distribution of Dye Concentration with Respect to Cumulative Discharge	20
D. Conservation of Mass	20
V. INTERPRETATION OF RESULTS	25
VI. NUMERICAL SIMULATION OF TRANSVERSE MIXING PROCESS	29
A. Mathematical Model	29
B. Representation of the River as a Set of Stream Tubes	31
C. Determination of Concentration Distribution and Transverse Mixing Coefficients by the Simulation Method	35
VII. THE TRANSVERSE MIXING COEFFICIENT	36
A. As Determined by Simulation Method	36
B. As Determined by the Method of Moments	41
VIII. SUMMARY AND CONCLUSIONS	43
REFERENCES	46

LIST OF TABLES

Page No.

Table 1.	Distribution of Dye in Discharge Canal	14
Table 2.	Recovery Ratios Determined from Experimental Data	25

LIST OF FIGURES

Figure 1.	Site plan for Cooper Nuclear Station	2
Figure 2.	Map of test reach showing location of dye sampling transects	4
Figures 3a-3f.	Transverse distributions of depth, velocity and unit discharge at:	
	3a. Mile 532.23	6
	3b. Mile 531.5	7
	3c. Mile 530.5	8
	3d. Mile 529.0	9
	3e. Mile 527.5	10
	3f. Mile 526.11	11
Figure 4a-4b.	Photographs showing:	
	4a. Mariotte tank introducing dye into circulating-water system	12
	4b. Dye sample being taken from river	12
Figures 5a-5d.	Transverse distributions of dye concentration:	
	5a. Transects 1 and 2	15
	5b. Transects 3 and 4	16
	5c. Transects 5, 6 and 7	17
	5d. Transects 8, 9 and 10	18
Figures 6a-6d.	Distribution of dye concentration with respect to normalized cumulative discharge:	
	6a. Transects 1 and 2	21
	6b. Transects 3 and 4	22
	6c. Transects 5, 6 and 7	23
	6d. Transects 8, 9 and 10	24
Figure 7.	Excess temperature isotherms based on dye experiment for $Q = 56,100$ cfs	26
Figure 8.	Comparison between excess temperature isotherms based on dye experiment, and isotherms predicted by AEC Battelle NW for reference design, at $Q = 35,000$ cfs	28

Figure 9.	Definition sketch for stream tubes	32
Figure 10.	Relative unit discharge versus relative depth relationship for synthesizing transverse distribution of unit discharge	34
Figure 11.	Variation of transverse mixing coefficient along test reach as determined by simulation method	37
Figures 12a-12c.	Comparison between simulated and measured transverse concentration distributions:	
	12a. Transects 3 and 4	38
	12b. Transects 5, 6, and 7	39
	12c. Transects 8, 9, and 10	40
Figure 13	Variance, $\sigma_{q_c}^2$, as a function of longitudinal distance	44

LIST OF SYMBOLS

C	Dye concentration in parts per billion by weight (ppb).
\bar{C}^d	Depth-averaged dye concentration (ppb).
C_E	Dye concentration in discharge canal effluent (ppb).
C_m	Dye concentration in river for fully mixed condition (ppb).
$C_{i,j}$	Average dye concentration in i 'th longitudinal increment of j 'th stream tube (ppb).
d	Local depth in feet.
\bar{d}	Average depth in feet.
D	Transverse diffusion factor = $E_z \bar{u}^d d^2$ in ft^5/sec^2 .
E_z	Transverse mixing coefficient in ft^2/sec .
h_1	Metric coefficient which corrects longitudinal distances for curvature in channel alignment.
i,j	Indices for longitudinal and transverse distance increments in finite difference scheme.
q	Local river discharge per unit width in ft^2/sec .
\bar{q}	River discharge per unit width averaged across width of channel in ft^2/sec .
q_c	Cumulative river discharge from the Nebraska side in ft^3/sec (cfs).
q_s	Flow discharge in a single stream tube in cfs.
Q_E	Effluent discharge from discharge canal in cfs.
Q_R	Total river discharge in cfs.
RR	Recovery ratio, i.e. ratio of dye flux measured in river to dye flux introduced into circulating water system.

T_a	Ambient temperature of river water in °F.
u, v, w	Local time-averaged flow velocity in x, y and z directions respectively in ft/sec.
\bar{U}	Velocity of flow averaged over channel cross section in ft/sec.
\bar{u}^d	Local depth-averaged velocity of flow in ft/sec.
u_*	Shear velocity = \sqrt{gdS} , where g = acceleration of gravity and S = energy gradient, in ft/sec.
W	Width of channel in feet.
x, y, z	Distances in longitudinal, vertical and transverse directions respectively, in feet.
ϵ_y, ϵ_z	Local turbulent mass transfer coefficients for y and z directions in ft ² /sec.
σ_c^2	Variance of distribution of dye tracer with respect to cumulative river discharge in ft ⁶ /sec ² .

TRANSVERSE MIXING CHARACTERISTICS OF THE
MISSOURI RIVER DOWNSTREAM FROM
THE COOPER NUCLEAR STATION

I. BACKGROUND

At the request of the Nebraska Public Power District, an experiment was performed to investigate the transverse mixing characteristics of the Missouri River in the reach immediately downstream from the Cooper Nuclear Station, near Brownville, Nebraska. The purpose of the investigation was to test the adequacy of the present discharge-canal system for accomplishing sufficient mixing to meet the temperature standards set by the regulatory agencies for this section of the Missouri River. According to the standards as tentatively formulated, the temperature of the water in the river may not be increased by more than 5°F except within a mixing zone of undefined shape that is not larger than 45 acres. Also the temperature is not to exceed 90°F at any time except by natural causes.

The circulating-water system of the Cooper Nuclear Station together with the service-water system is designed to withdraw a flow of 1,455 cubic feet per second (cfs) from the river through the intake structure, and return it through the discharge canal. The site plan, including the layout of the intake structure and the discharge canal, is shown in Fig. 1. When operating at the full load of 800 mw, the temperature rise across the plant will be 18°F. Therefore the required dilution to be obtained in the mixing zone is 18/5, except when the ambient temperature T_a exceeds 85°F in which case the required dilution is $18/(90-T_a)$.

In the experiment, the fluorescent dye, Rhodamine WT, was used as a tracer to simulate the heated effluent. The dye tracer, which was neutrally buoyant and conservative, did not simulate the heated effluent in either buoyancy effects or heat transfer to the atmosphere. However, calculations based on the results of Prych (1970) show that the buoyancy effects should be negligible in the Missouri River for both summer and winter conditions.

MISSOURI RIVER

FLOW →

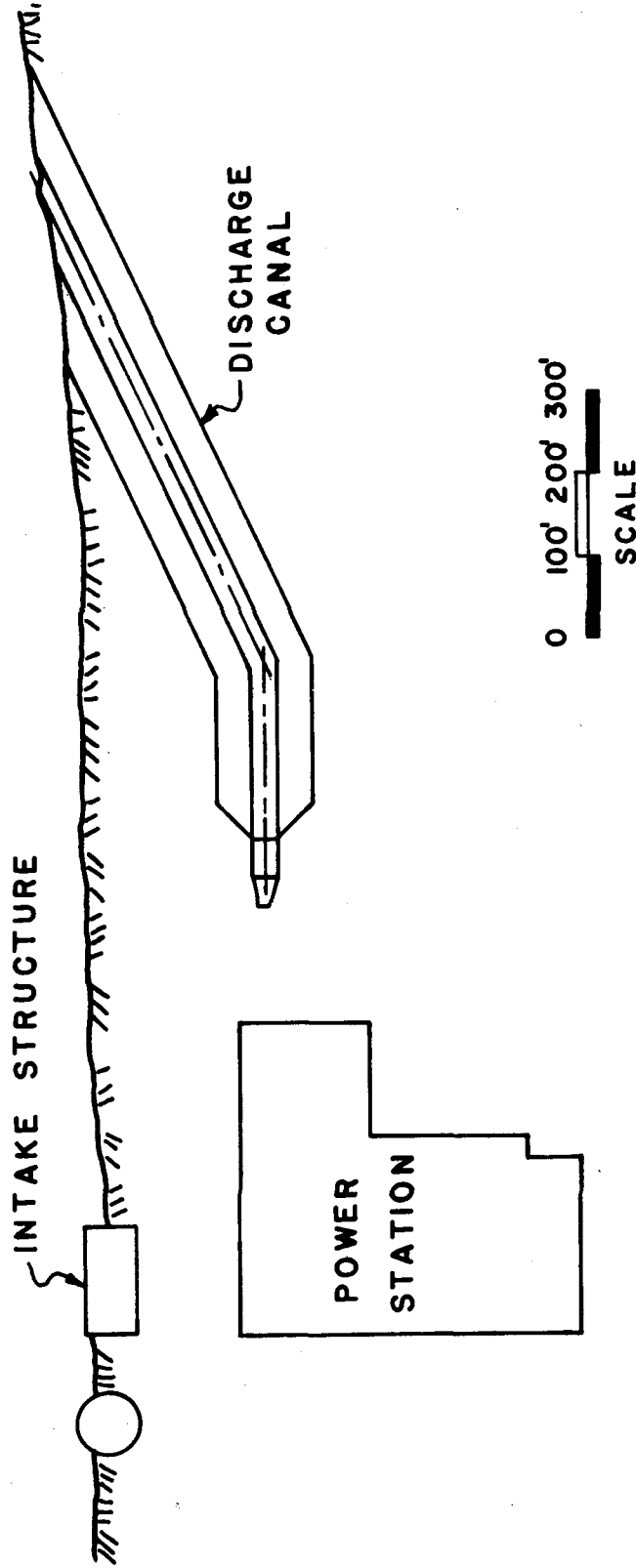


Fig. 1.— Site plan for Cooper Nuclear Station

Calculations based on the work of Ryan and Stolzenbach (1972) show that the heat transfer to the atmosphere in the test reach should also be negligible for most conditions. For example, assuming a water surface temperature of 85°F, an air temperature of 60°F, a wind velocity of 30 mph and a relative humidity of 40 percent, which would collectively produce a much higher than normal rate of heat transfer, the computed heat loss in the six-mile test reach, assuming a normal summer river flow of 30,000 cfs, does not amount to more than about 8 percent of the excess heat at full plant load. At lower river discharges the percent of heat loss would tend to be somewhat higher, due mainly to the longer flow-through time.

Participants in the investigation included personnel from the Institute of Hydraulic Research of The University of Iowa, Industrial Bio-Test Laboratories Inc., the Minnesota District Office of the Water Resources Division of the U.S. Geological Survey, and the Nebraska Public Power District. Overall supervision and coordination of the investigation was provided by the Iowa Institute of Hydraulic Research.

II. DESCRIPTION OF TEST REACH

The Cooper Nuclear Station is located on the west bank of the Missouri River at Mile 532.5 near the downstream end of the Lower Brownville Bend. The test reach extends downstream to Mile 526.11 and includes the Langdon and Aspinwall Bends. The channel is constrained by a system of dikes and jetties to a width of about 700 to 900 feet, and an alignment consisting of a series of smooth curves. A map of the test reach is shown in Fig. 2. The channel bottom consists predominantly of sand, having a median diameter of 0.25 mm. The slope of the test reach is about 0.00019. During the navigation season the river discharge is maintained at not less than about 30,000 cfs. During the winter the discharge may be considerably less; in recent years it has not dropped below about 6,500 cfs. Depending on river discharge and temperature, either a dune-or plane-bed configuration may exist. In an extensively-studied reach near Omaha, a dune-bed configuration which is typical for the spring and summer months, characteristically gives way to a much smoother plane-bed configuration during the fall.

On the day of the experiment, October 11, 1972, the river discharges, measured 30 miles upstream from the test reach at Nebraska City, and 38

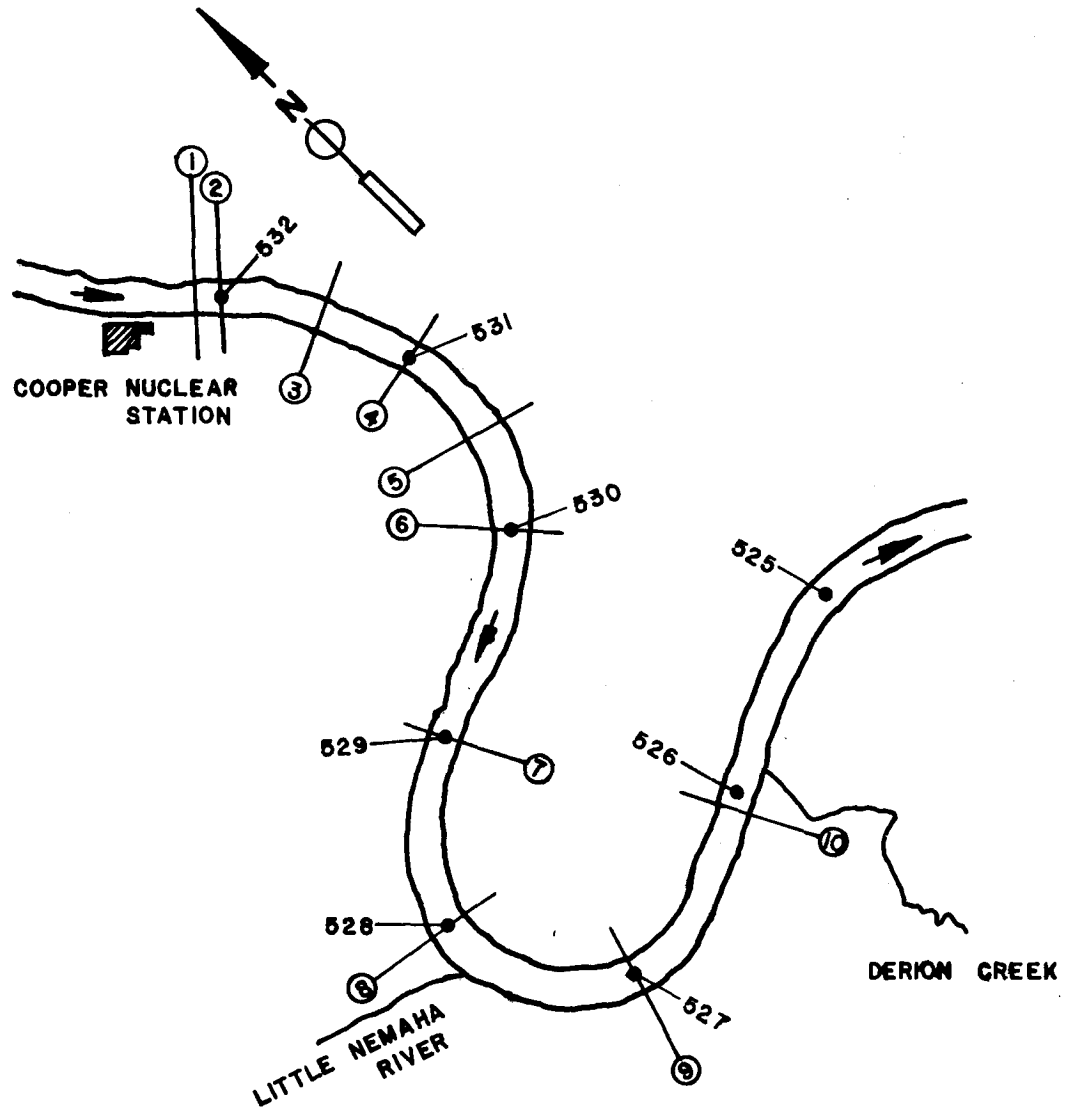


Fig. 2. — Map of test reach showing location of dye-sampling transects.

miles downstream at Rulo, were 56,100 cfs and 56,400 cfs. respectively. Because of greater tributary inflow between the test reach and Rulo, the former figure of 56,100 cfs was adopted. The average depth of the channel was about 13 ft., and of the thalweg about 22 ft.

The U.S. Geological Survey (USGS) party from Minnesota measured the transverse distribution of depth and velocity 3-ft below the surface by the moving boat method at six different cross sections on the day of the experiment. The results of these measurements are shown in Figs. 3a through 3f. In these figures d is the local depth, \bar{u}^d is the estimated local depth-averaged velocity, $q = \bar{u}^d d$ is the estimated local discharge per unit width, and $\bar{q} = Q_R/W$ is the discharge per unit width averaged across the width of the channel, where Q_R = river discharge, and W is the width of the channel.

III. DESCRIPTION OF EXPERIMENT

A. Dye Introduction. The tracer solution was obtained by mixing equal volumes of the commercially available DuPont Rhodamine WT solution (specific gravity = 1.19, concentration by weight = 20%), and methyl alcohol (specific gravity = 0.81) with sufficient water to obtain a dye concentration of 0.05 in the mixture. The tracer solution was introduced directly into the circulating-water system of the plant from two Mariotte tanks, made from 55-gallon drums, by gravity flow through hoses into the intake bays of the No.1 and No. 3 pumps. Fig. 4a shows one of these Mariotte tanks in place. The hoses were attached to weighted cables so that the lower ends of the hoses were at about the same level as the pump intakes. The combined flow from the two tanks was maintained at an average rate of 30.4. ml/sec from 0800 hours until 1333 hours. The flow rates were monitored at intervals of about one-half hour with a stop watch and graduated cylinder throughout the course of the experiment. Variations of up to 7 percent of the mean flow rate were observed. No satisfactory explanation for this variation has been found. During calibration tests with water, there was no perceptible variation. Both tanks had to be refilled once during the experiment. During the down times the average flow rate was maintained by manually feeding in the required amounts at about two-minute intervals. The dye-introduction operation was designed and performed by personnel from the Iowa

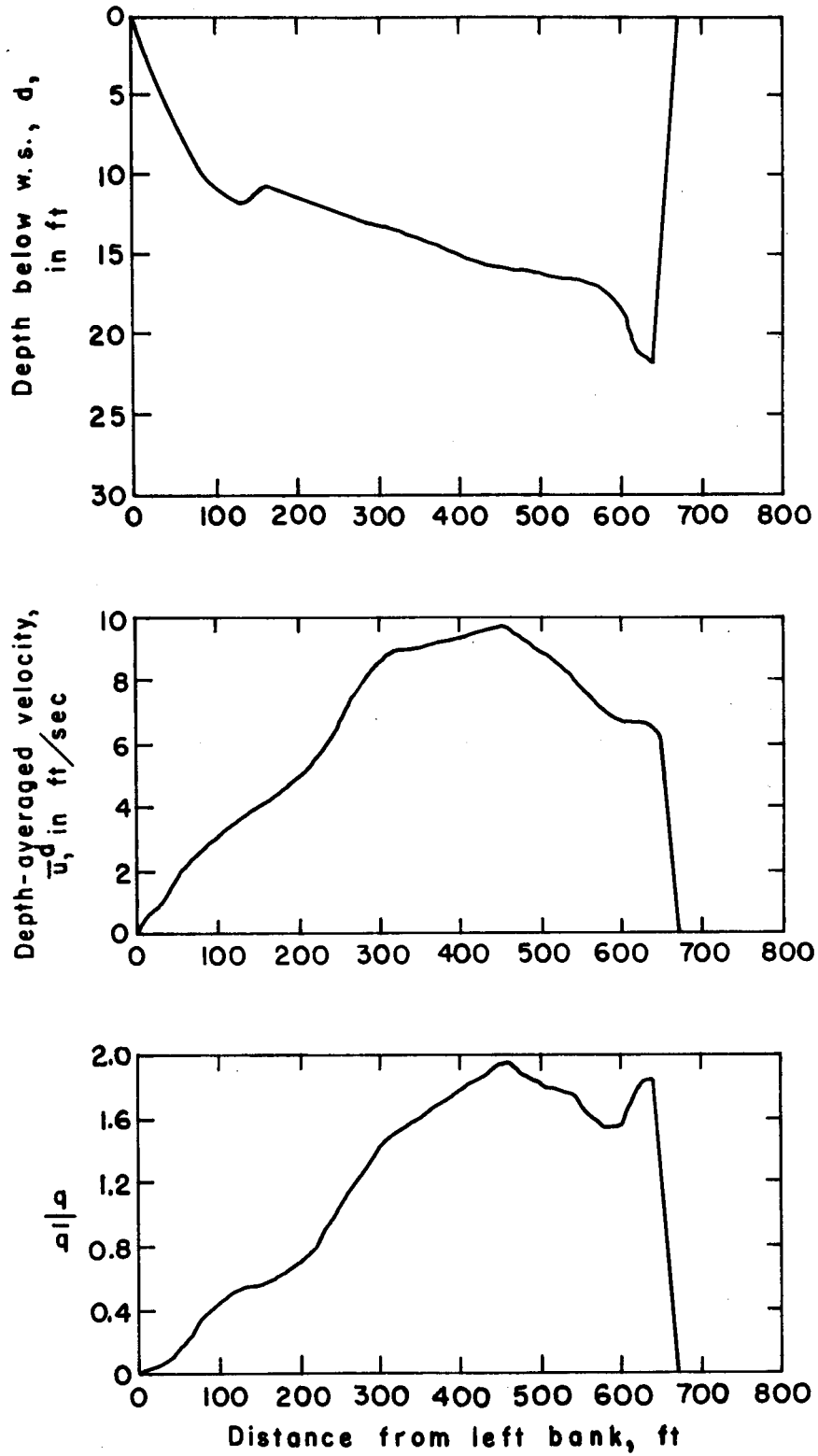


Fig. 3a. — Transverse distribution of depth, velocity and unit discharge at Mile 532.23

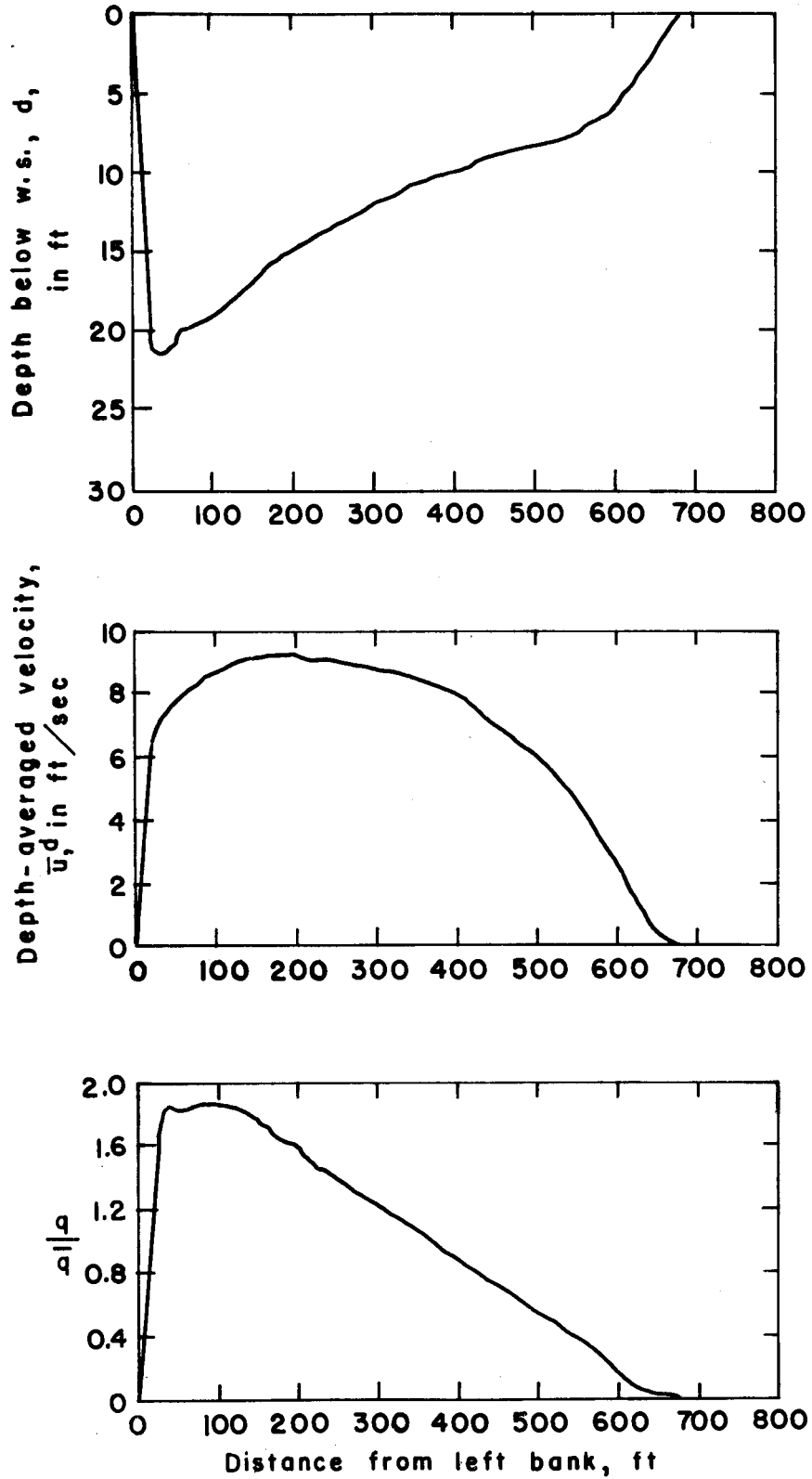


Fig. 3b.— Transverse distribution of depth, velocity and unit discharge at Mile 531.5

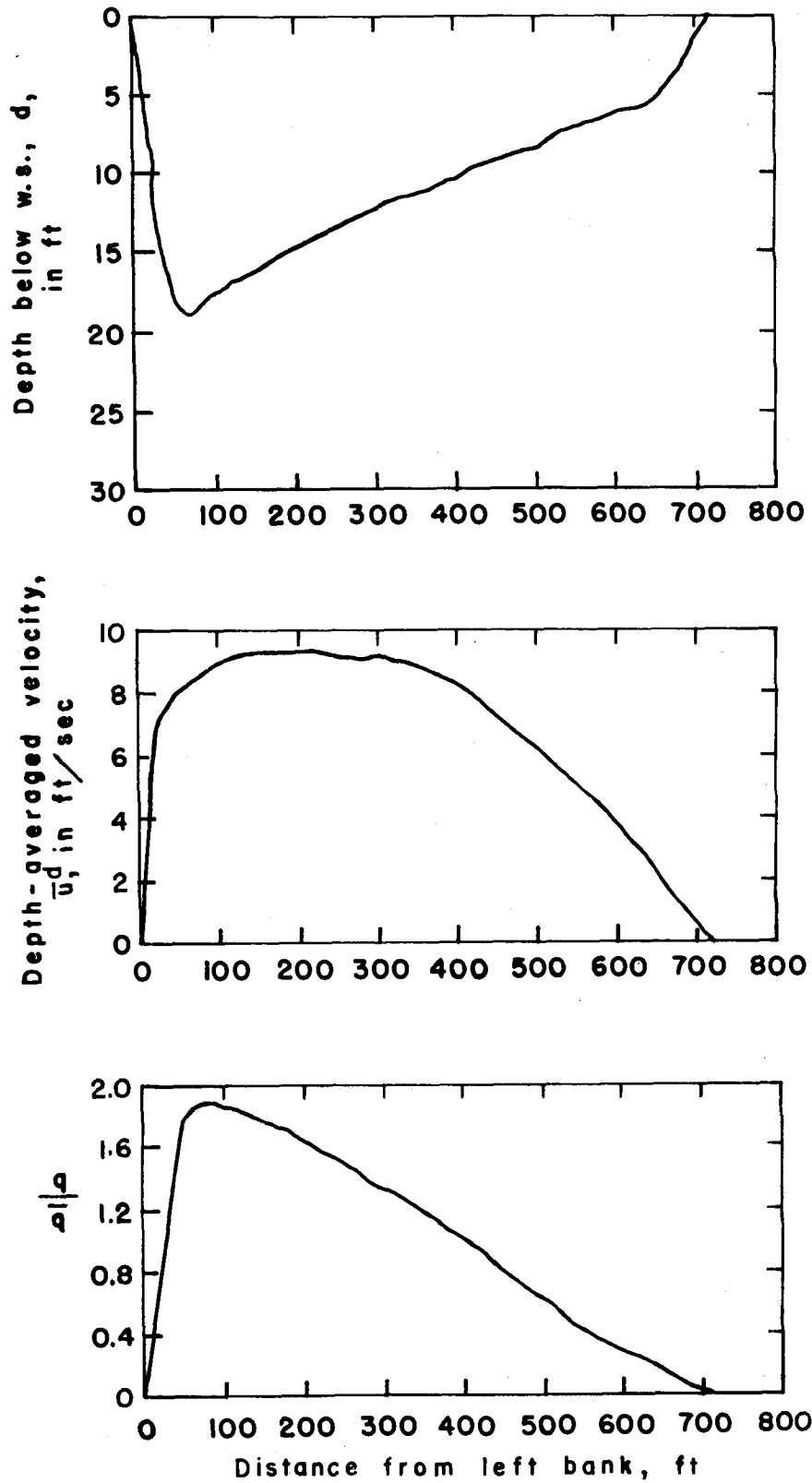


Fig. 3c. — Transverse distribution of depth, velocity and unit discharge at Mile 530.5

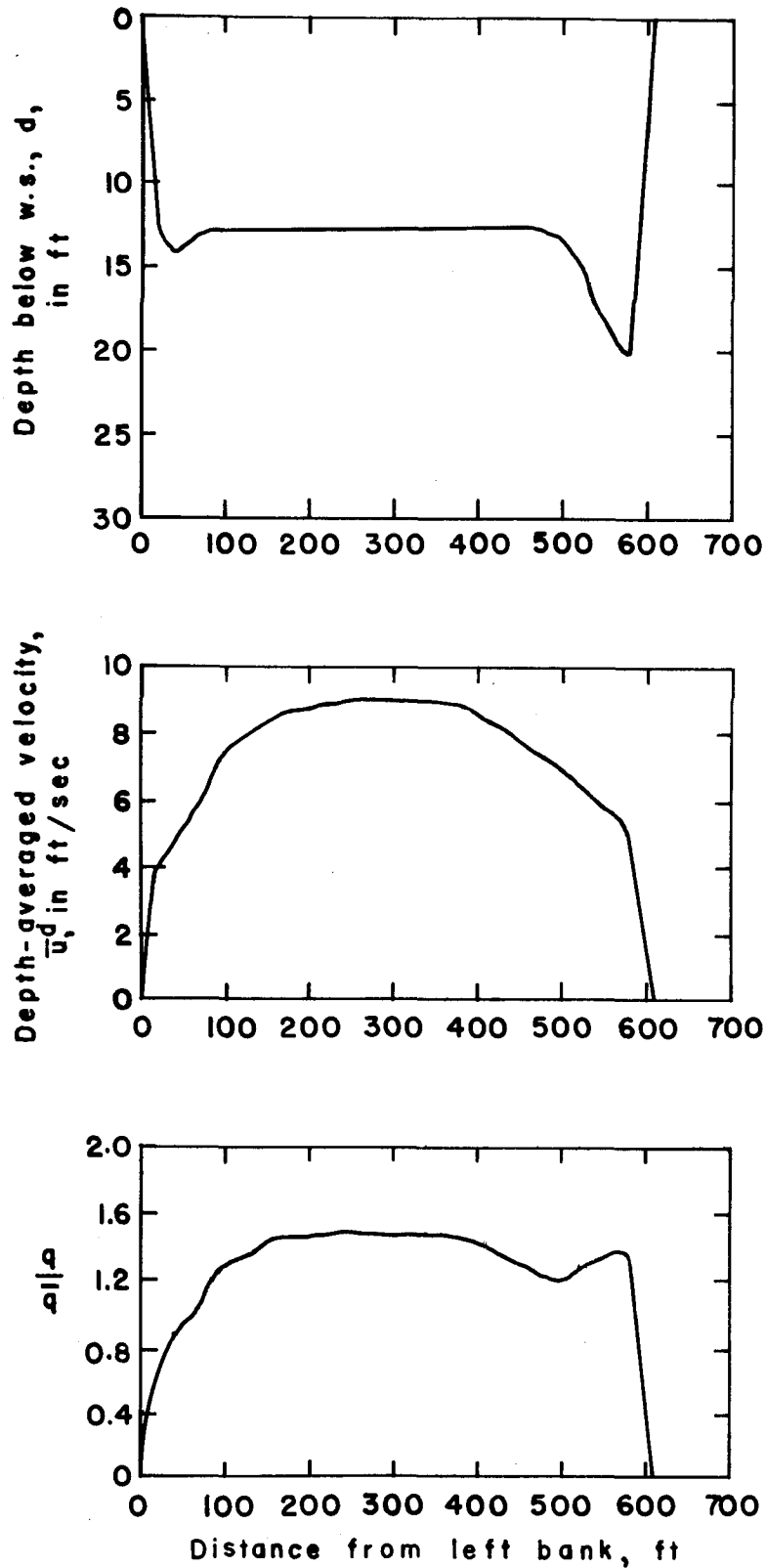


Fig. 3d. — Transverse distribution of depth, velocity and unit discharge at Mile 529.0

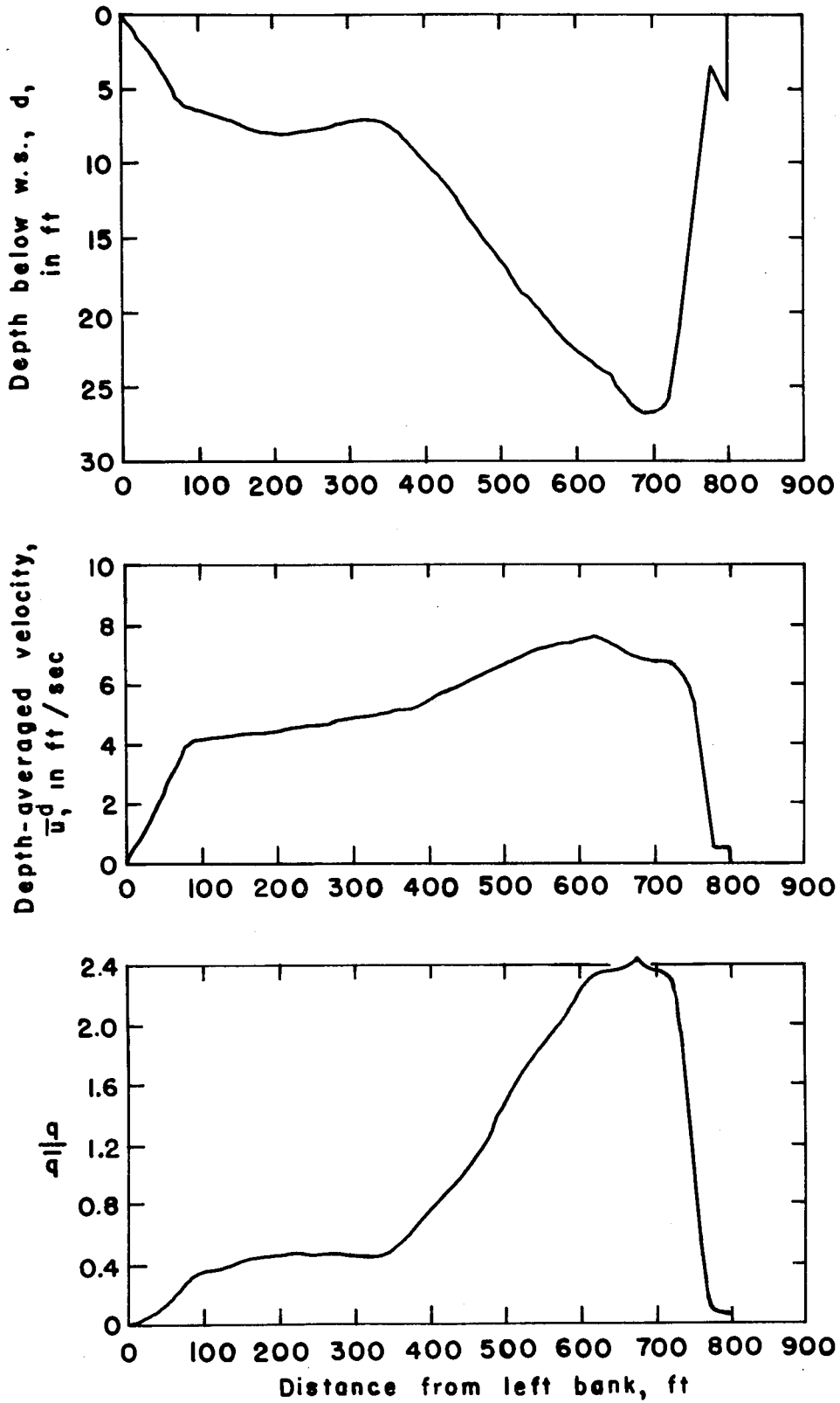


Fig. 3e. — Transverse distribution of depth, velocity and unit discharge at Mile 527.5

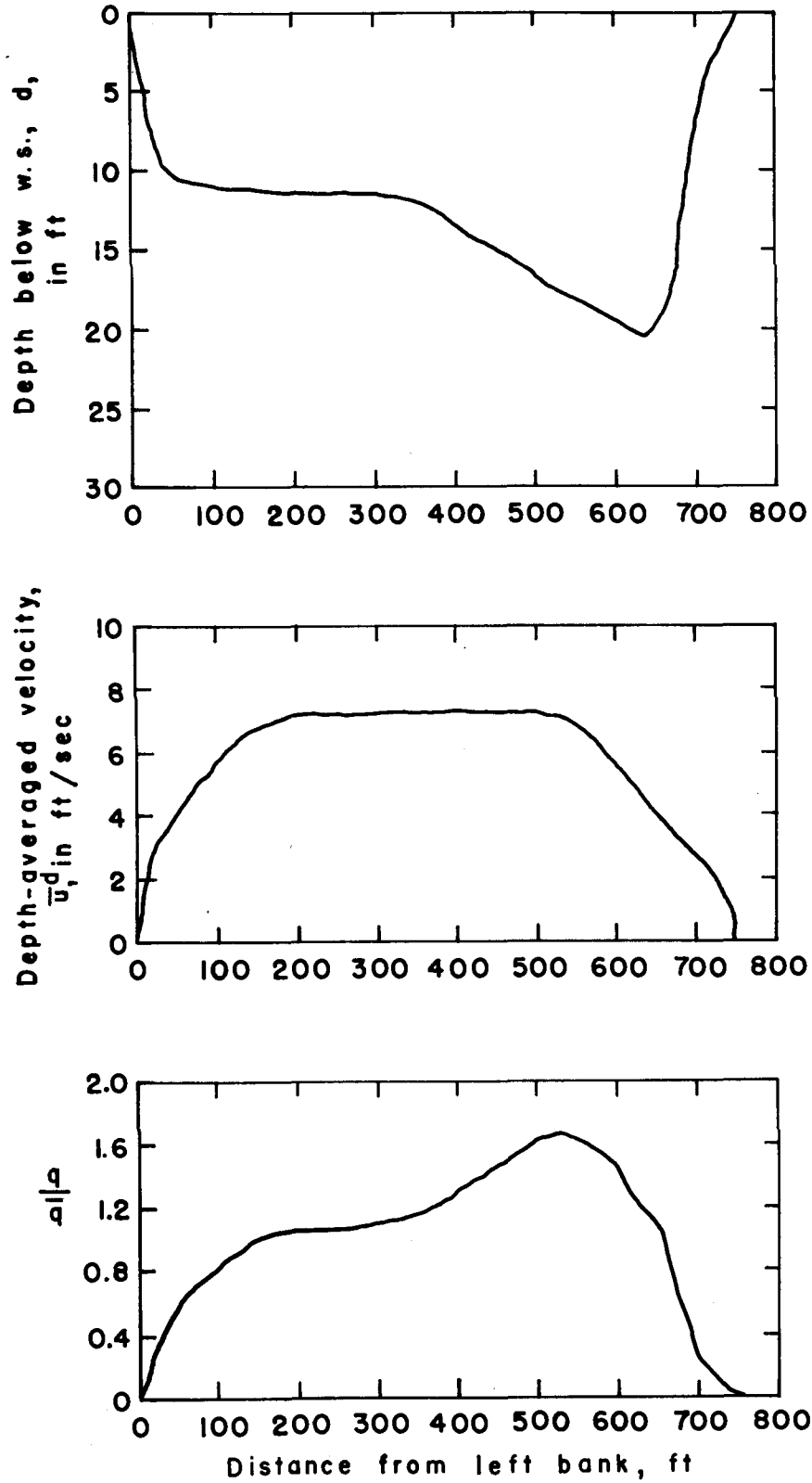


Fig. 3f.—Transverse distribution of depth, velocity and unit discharge at Mile 526.11

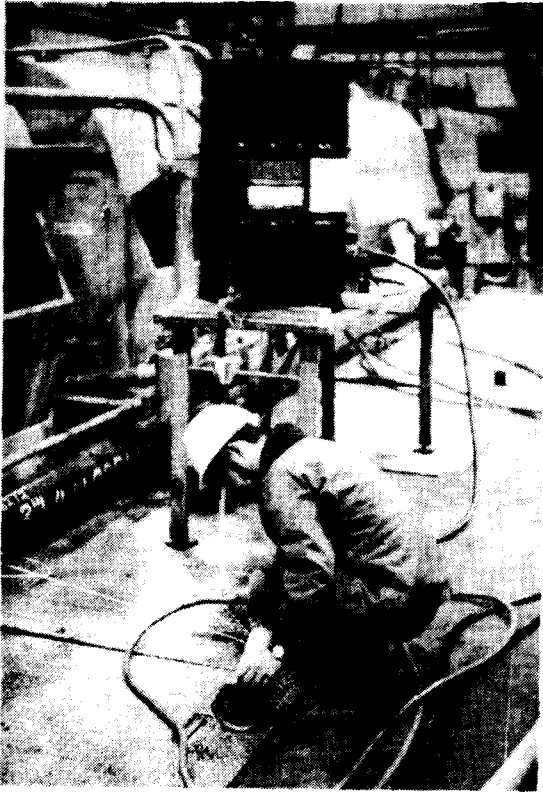


Fig. 4a. - Mariotte tank introducing dye into circulating water system



Fig. 4b. - Dye sample being taken from river

Institute of Hydraulic Research (IIHR) with the assistance of personnel from the Nebraska Public Power District (NPPD).

Throughout the experiment all four main pumps and the two service-water pumps were operating at a combined discharge of 652,000 gpm (1455 cfs). Assuming complete mixing in the circulating-water system and discharge canal, this discharge, together with the 30.4 ml/sec flow rate and 5% concentration of the tracer solution, give a theoretical dye concentration in the discharge canal of 36.8 parts per billion (ppb).

B. Sample Collection. The distribution of dye tracer across the channel at the ten cross sections, or "transects", indicated in Fig. 2 was determined in the same manner as by Yotsukura *et al* (1970). Briefly, discrete samples were taken from a boat by dipping small glass bottles into the water at from 20 to 30 points across each transect. Fig 4b shows a sample being taken. The boat was maintained on the sampling line by a spotter on shore, and the boat position as each sample was taken was fixed by triangulation using a transit located on shore at one end of a pre-measured baseline. The other end of the baseline was located on the same shore on the sampling line. The angle between the sampling line and the baseline was also pre-measured. Radio contact was maintained between the sampling party, the transit party, and the spotter. Barring errors in individual transit readings, it is estimated that the computed sampling positions are accurate to within a few feet. The sampling was started at Transect 1 at 0855 hours and completed at Transect 10 at 1315 hours. Approximately 15 to 20 minutes was required for sampling one transect.

The sampling party was made up of Industrial Bio-Test Laboratories personnel, and the transit party and spotter from NPPD and IIHR personnel. The sampling lines and baselines were set up and surveyed prior to the experiment by Bio-Test and NPPD personnel.

C. Analysis of Samples. Following the experiment the samples were taken to the Industrial Bio-Test Laboratories at Northbrook, Illinois, and analyzed for dye concentration with an Aminco-Bowman Spectrophotofluorometer. An excitation wavelength of 550 nm and an emission wavelength of 575 nm were used. The instrument was calibrated by obtaining fluorescence readings for standard solutions of known dye concentrations made up from samples of the tracer solution and river water. Samples of river water outside of the dye plume were taken to determine background readings.

IV. PRESENTATION OF RESULTS

A. Dye Distribution in the Discharge Canal. Nine samples were taken at the downstream end of the discharge canal starting at 0830 hours. The sampling positions and concentrations are shown in Table 1. The dye concentration was nearly uniform, and the average concentration of 35.6 ppb is close to the theoretical concentration of 36.8 ppb calculated from the concentration and flow rate of the tracer solution and the combined discharge of the circulating-water and service-water pumps, assuming complete mixing.

Table 1. Distribution of Dye in Discharge Canal

Sampling Location	Dye Concentration (ppb)
Near West Bank	Surface 36.1 Mid-Depth 35.6 Bottom 33.9
Near Centerline	Surface 35.0 Mid-Depth 36.1 Bottom 36.1
Near East Bank	Surface 36.1 Mid-Depth 35.0 Bottom 36.1

Average Concentration = 35.6 ppb

B. Transverse Distribution of Dye Concentration. The transverse distribution of dye concentration obtained at the 10 transects is shown in Figs. 5a through 5d. The abscissa z/W represents the fraction of the total channel width measured from the Nebraska side. The average background reading, which corresponds to a dye concentration of 1.6 ppb, was subtracted from the spectrophotofluorometer readings before the data were plotted. The temperature scale on the right-hand ordinate is based on the assumption that a dye concentration of 36 ppb in the discharge canal is equivalent to an excess temperature of 18°F.

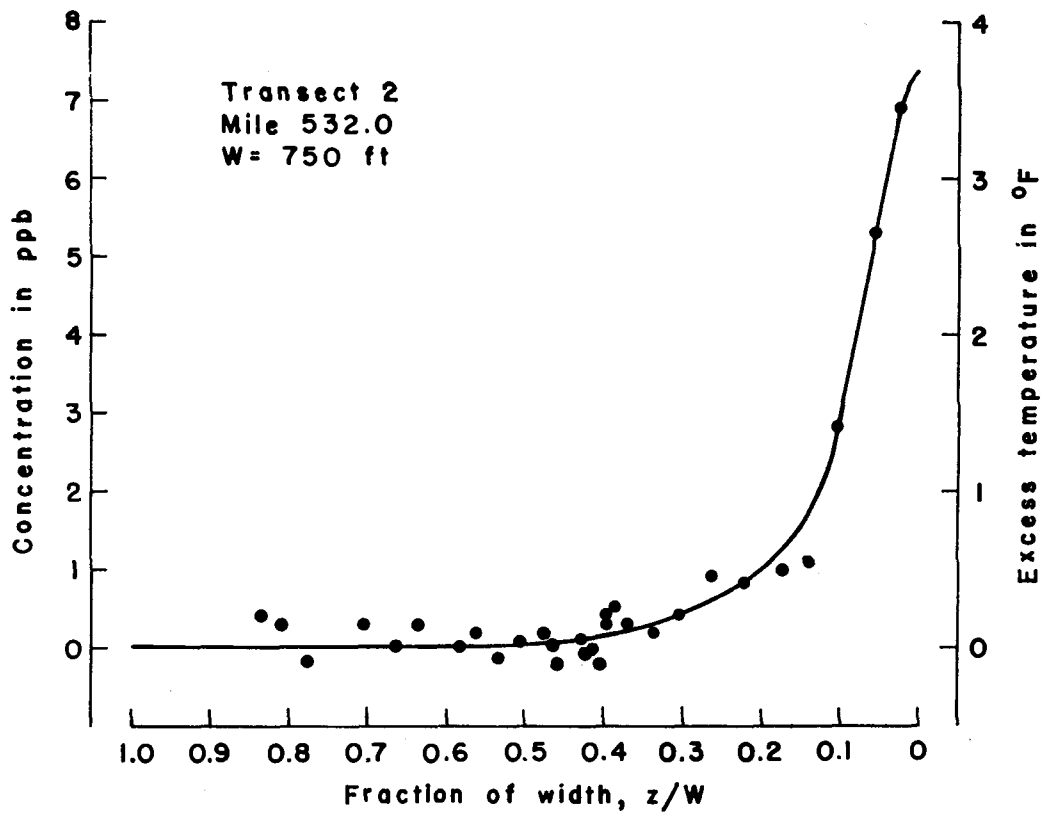
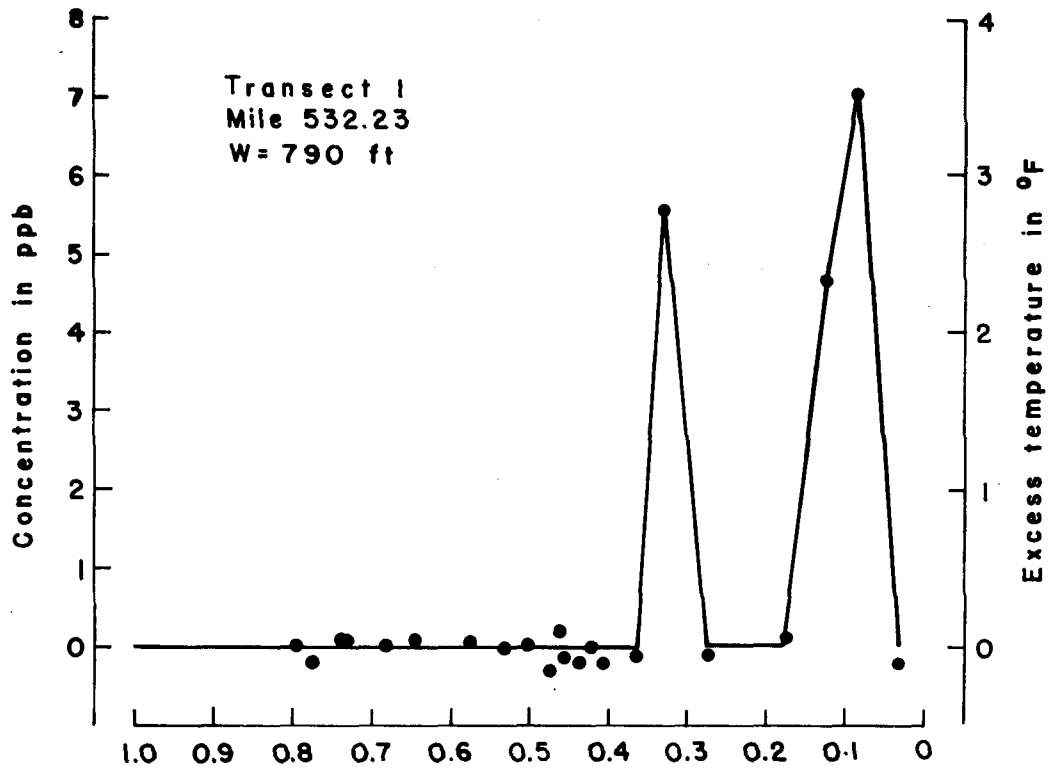


Fig. 5a.—Transverse distribution of dye concentration, Transects 1 and 2

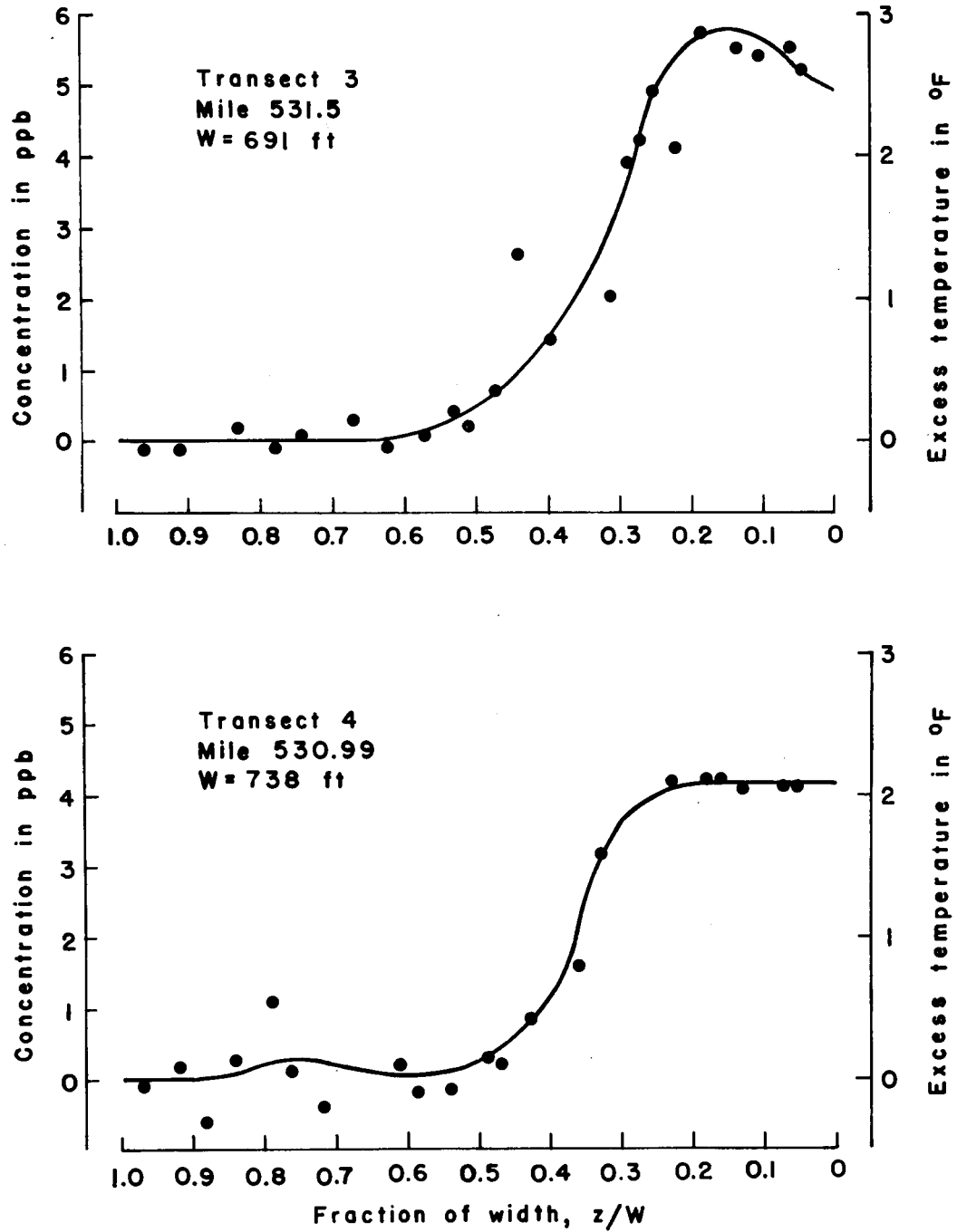


Fig. 5b.—Transverse distribution of dye concentration, Transects 3 and 4

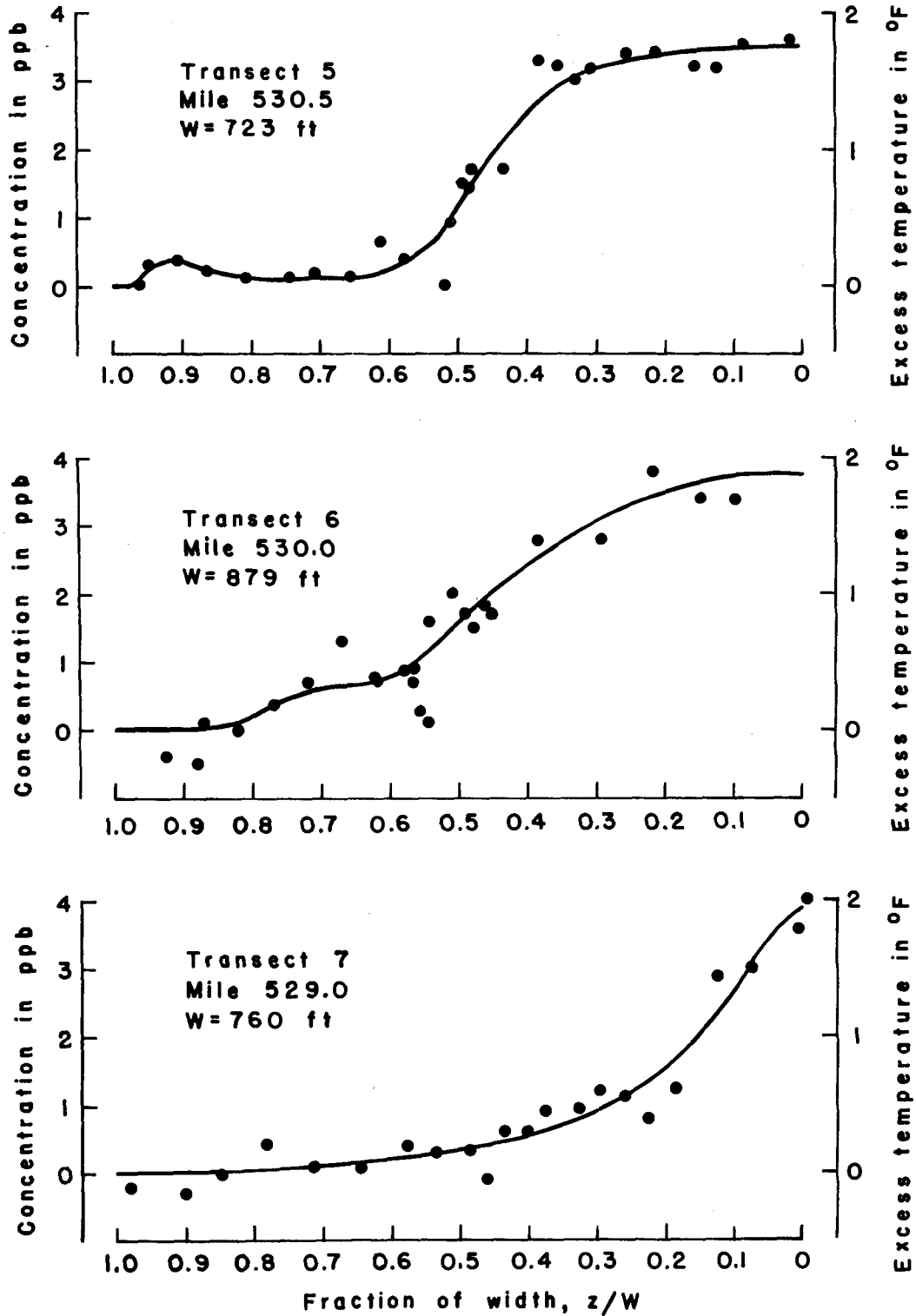


Fig. 5c.—Transverse distribution of dye concentration, Transects 5, 6 and 7

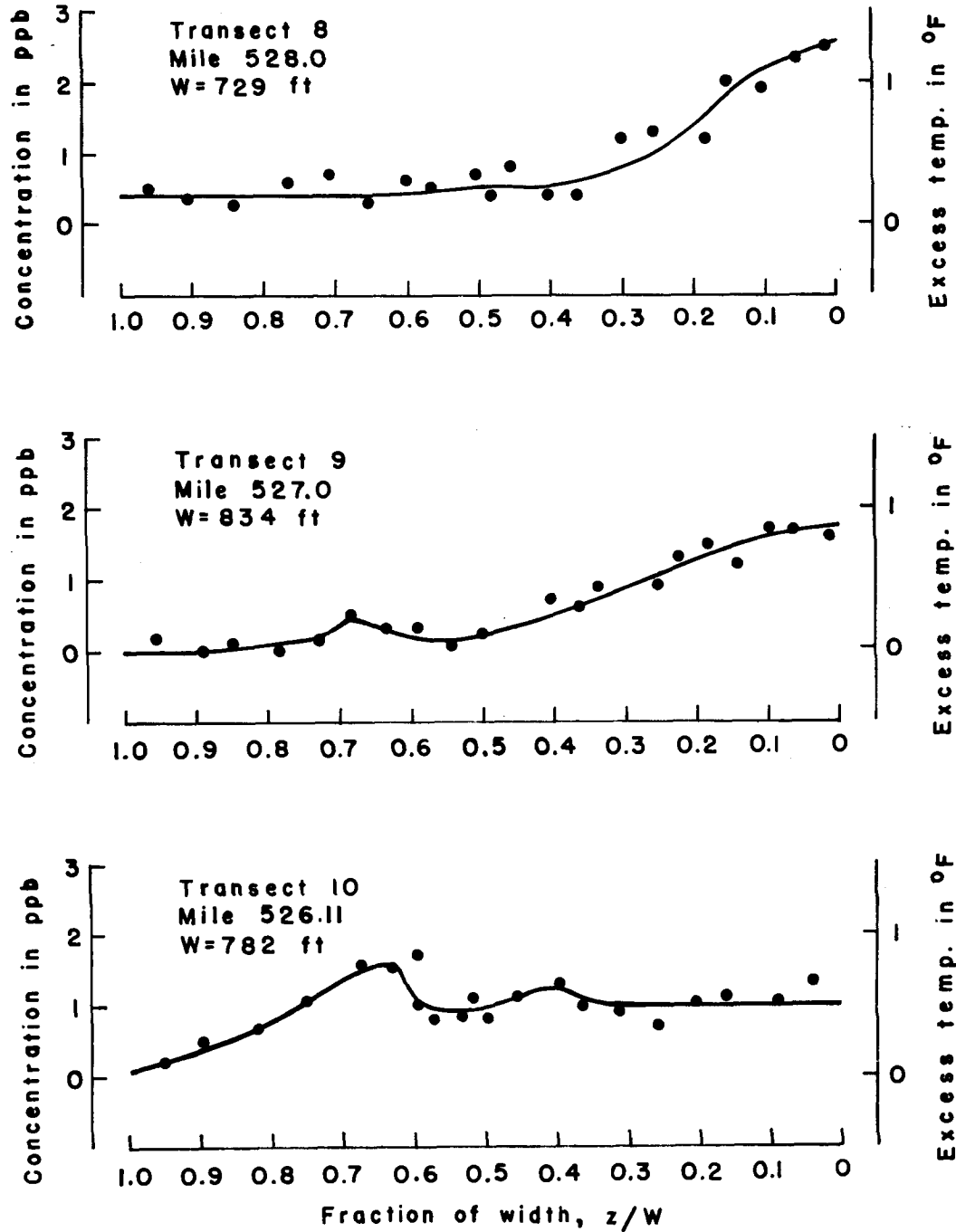


Fig. 5d.—Transverse distribution of dye concentration, Transects 8, 9 and 10

The data show that the dye spreads gradually across the river so that at Transect 10, 6.15 miles downstream from the end of the discharge canal, it is spread nearly all the way across. The overall rate of transverse spreading, defined here as the increase in the variance of the transverse distribution per unit of longitudinal distance, is approximately six times that observed by Yotsukura *et al* (1970), in the reach downstream from Blair, Nebraska, 116 miles further upstream. At the time of the Blair experiment in November, 1967, the river discharge was approximately 40 percent less. The faster spreading in the present experiment is attributed more to the difference in the sinuosity of the two reaches than to the difference in river discharge. The curvature in alignment in the Brownville reach is much more pronounced, and would cause a correspondingly greater rate of transverse mixing due to bend-generated secondary currents.

The scatter of the data points is attributed to the combined effect of the randomness of the mixing process, the discrete sampling procedure, and the variation of background fluorescence. In the vicinity of Transect 1 patches of water having a high dye concentration interspersed with patches having a low- or zero-concentration were visible to the naked eye. The transverse distribution with the two spikes shown for Transect 1 undoubtedly reflects this randomness and is almost certainly not a representative distribution. More samples at a closer spacing should have been taken in the dye plume. With increasing distance downstream the randomness became less pronounced so that the concentration profiles became better defined, but the variation in background fluorescence persisted. For some unexplained reason, the level and variation of background fluorescence was about sixfold greater in this experiment than in the Blair experiment.

During the time interval between sampling at Transect 4 and sampling at Transect 5, a large string of barges passed by, going in the upstream direction close to the Missouri shore. Sampling at Transect 5 was not started until one-half hour after the barges had gone by. If the barges had any significant effect on the transverse mixing of the dye, the effect is not clearly evident. The effect could have been substantial if, for example, the barges had crossed over to the Nebraska side and passed through the dye plume in the region where it was still fairly concentrated.

C. Distribution of Dye Concentration with Respect to Cumulative Discharge. In Figs. 6a through 6d, dye concentration is plotted as a function of the normalized cumulative discharge from the Nebraska side in the manner proposed by Yotsukura and Cobb (1972). The normalized cumulative discharge is defined as

$$\frac{q_c}{Q_R} = \frac{1}{Q_R} \int_0^z q \, dz \quad (1)$$

An advantage of using q_c/Q_R , which may be thought of as a flux-weighted relative distance, rather than the unweighted relative distance z/W as the independent variable, is that it provides a more accurate description of the actual mixing process in nonuniform, meandering channels such as the Missouri River. As shown in Figs. 3a through 3f the thalweg zone, where the flow is most highly concentrated, wanders back and forth across the channel, providing a mechanism for lateral convective transport which, unlike lateral turbulent transport, does not necessarily imply mixing. Representing concentration as a function of q_c/Q_R reflects only the mixing, whereas representing concentration as a function of z/W reflects the mean lateral convective-transport mechanism as well.

The normalized cumulative discharge as a function of z/W for the different transects was determined from the USGS data in Figs. 3a through 3f. The data were used directly for Transects 1, 3, 5, 7 and 10. For the other transects, transverse distributions of q/\bar{q} were synthesized, using depth soundings from a Corps of Engineers Hydrographic Survey (1967) together with q/\bar{q} distributions for similarly-shaped cross sections.

D. Conservation of Mass. According to the conservation of mass principle the total flux of dye through any cross section is

$$Q_E C_E = Q_R C_m = \int_0^W q \bar{C}^d \, dz = Q_R \int_0^1 \bar{C}^d \, d\left(\frac{q_c}{Q_R}\right), \quad (2)$$

where Q_E = flow in discharge canal (1455 cfs); C_E = dye concentration in discharge canal (36.8 ppb); Q_R = river discharge (56,100 cfs); C_m = fully - mixed dye concentration (0.95 ppb); and \bar{C}^d = depth-averaged local dye concentration. Values of the recovery ratio

$$RR = \frac{1}{Q_E C_E} \int_0^W q C \, dz \quad (3)$$

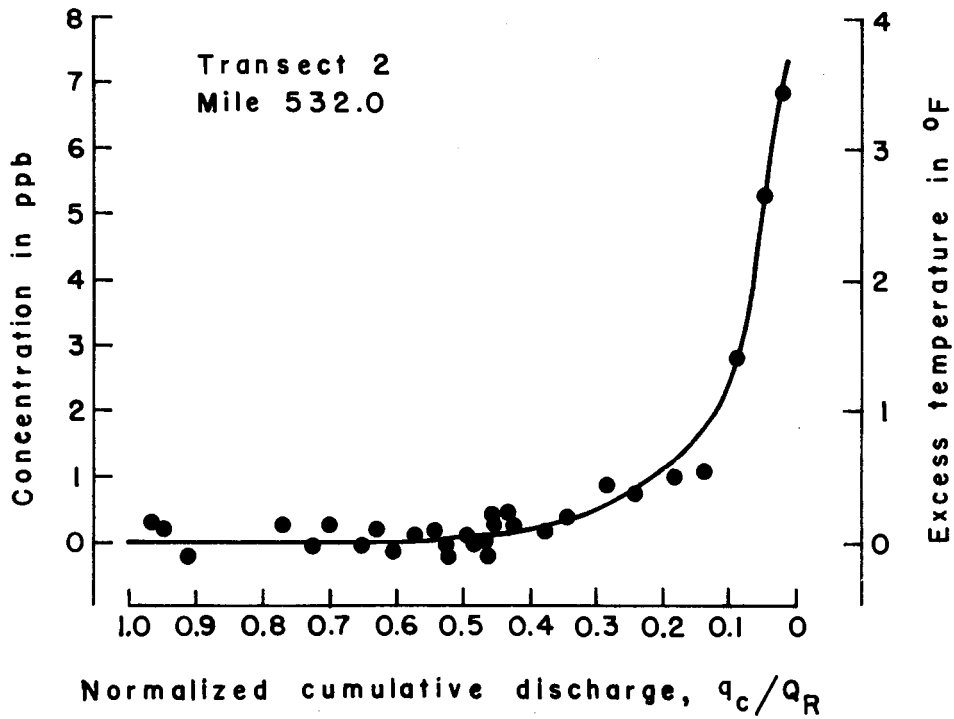
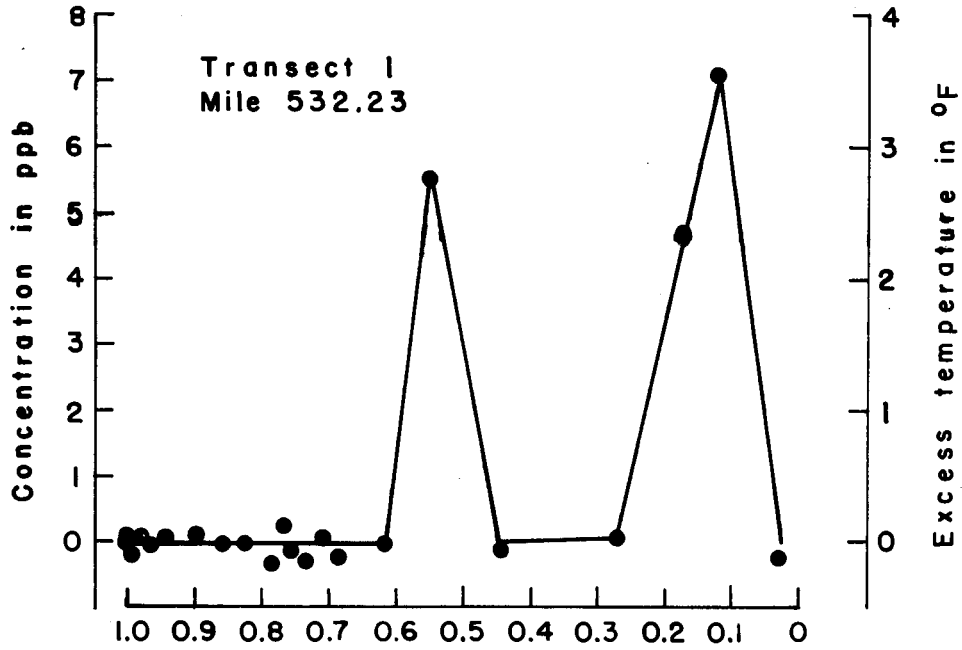


Fig. 6a.—Distribution of dye concentration with respect to normalized cumulative discharge, Transects 1 and 2

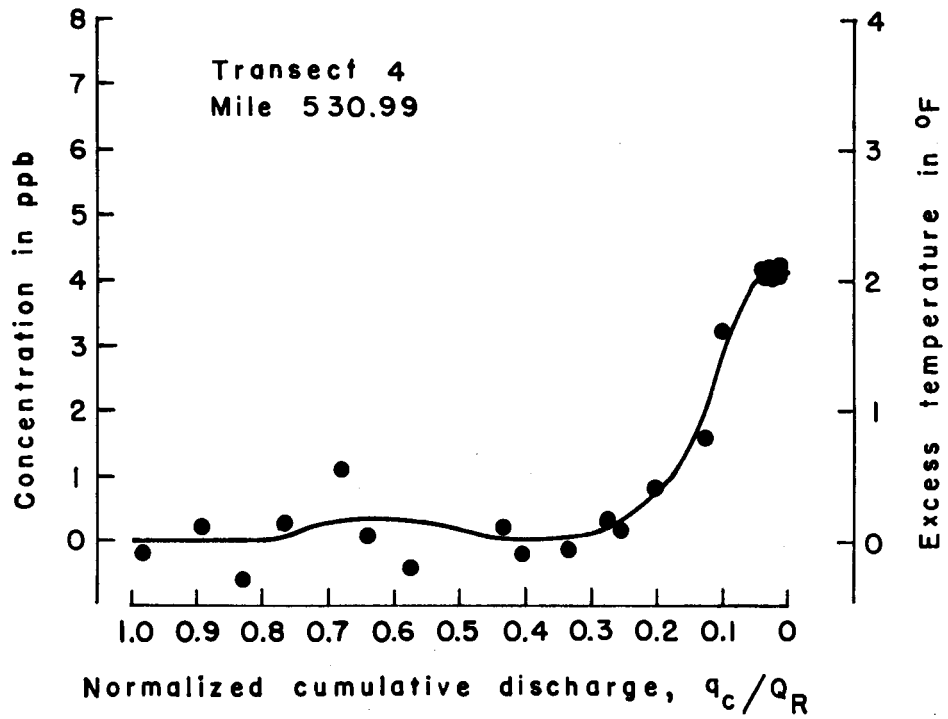
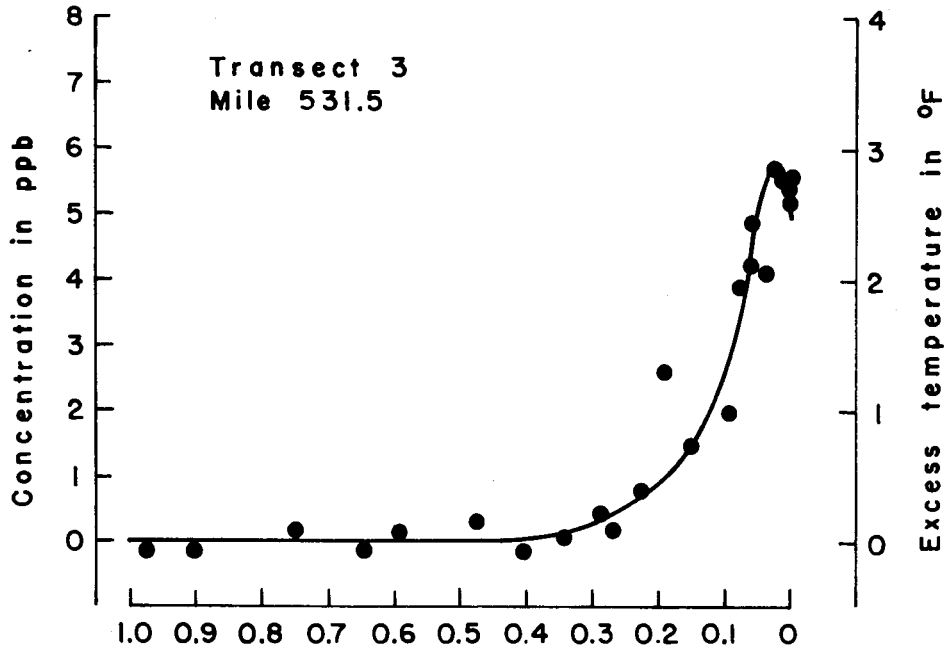


Fig. 6b.—Distribution of dye concentration with respect to normalized cumulative discharge, Transects 3 and 4

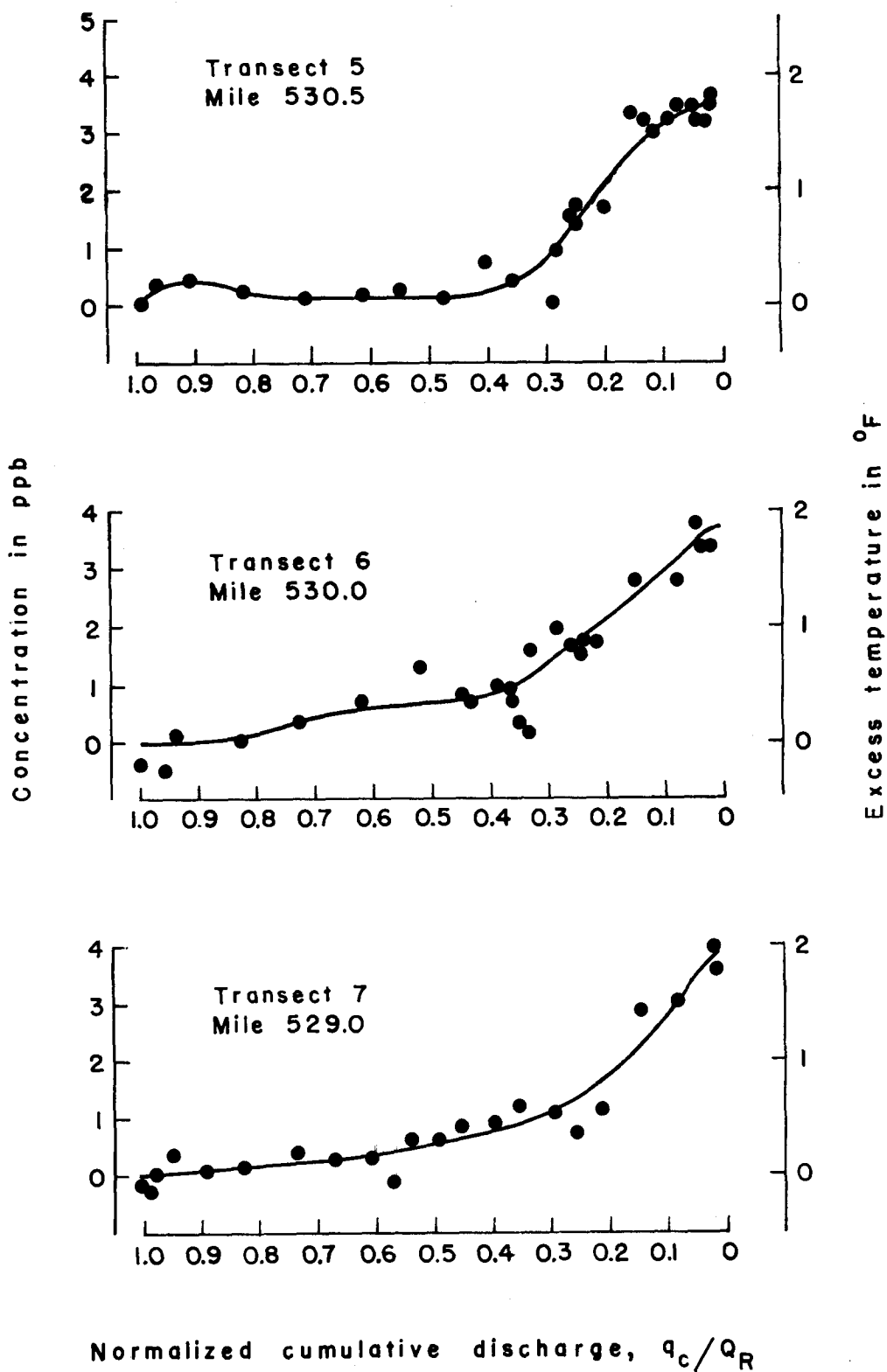


Fig. 6c. — Distribution of dye concentration with respect to normalized cumulative discharge, Transects 5, 6 and 7

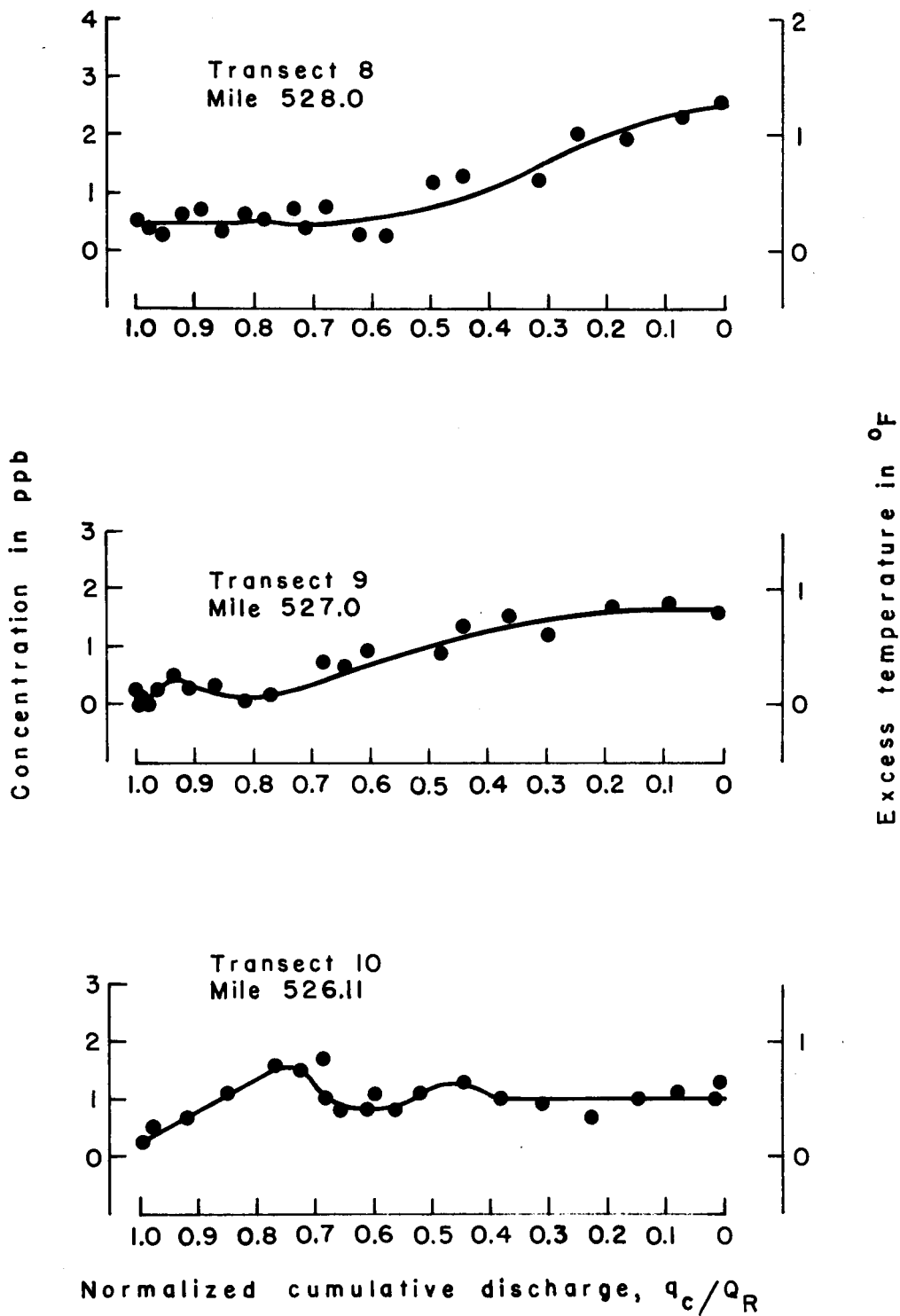


Fig. 6d.—Distribution of dye concentration with respect to normalized cumulative discharge, Transects 8, 9 and 10

and

$$RR = \frac{Q_R}{Q_E C_E} \int_0^1 C d\left(\frac{q_C}{Q_R}\right) \quad (3a)$$

determined from the data in Figs. 5a-5d and 6a-6d are shown for Transects 2-10 in Table 2. In the experimental determination of RR from Eqs. 3 and 3a, C = local concentration near the surface, not the depth-averaged concentration.

Table 2. Recovery Ratios Determined from Experimental Data

Transects	Recovery Ratio		Distribution of q
	Eq. 3	Eq. 3a	
2	0.75	0.77	Synthesized
3	0.72	0.70	Measured
4	0.70	0.66	Synthesized
5	0.90	0.92	Measured
6	1.14	1.13	Synthesized
7	0.98	1.00	Measured
8	1.19	1.21	Synthesized
9	1.01	1.01	Synthesized
10	1.05	1.05	Measured

If there is no dye loss, and representative samples are obtained, the value of the recovery ratio should equal one. Among the factors probably contributing to the deviation from this value are: (1) concentrations in samples, which were obtained near the water surface, may not have been representative of depth-averaged concentrations; (2) poor estimates of transverse q distributions, particularly where they were synthesized; and (3) variation of background fluorescence.

V. INTERPRETATION OF RESULTS

If heat transfer to the atmosphere is neglected, and it is assumed that an excess temperature of 18°F in the discharge canal is equivalent to a dye concentration of 36 ppb, and also that buoyancy effects are negligible, the excess temperature isotherms for the condition of full plant load and a river discharge of 56,100 cfs would be as shown in Fig. 7.

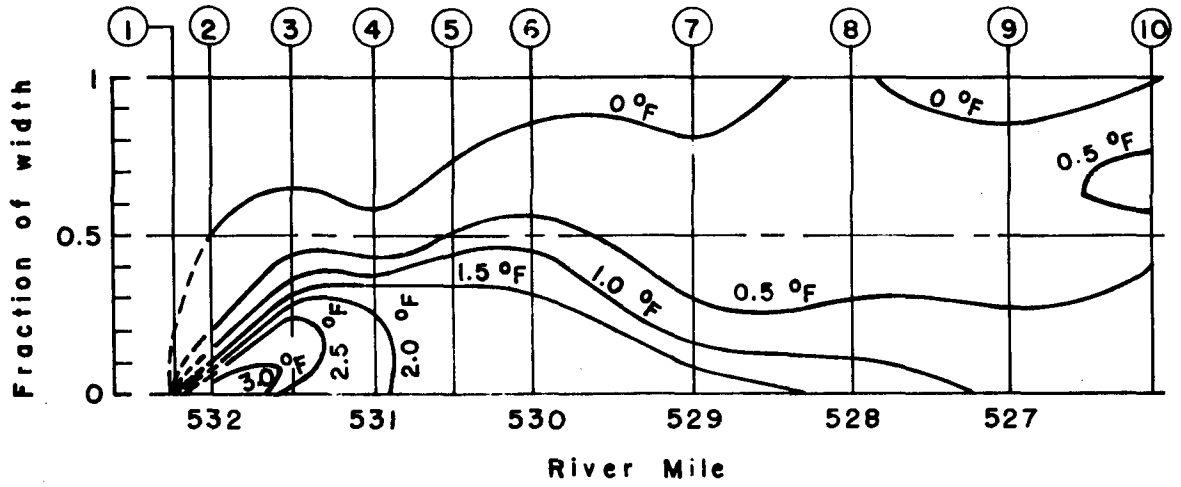


Fig. 7.— Excess temperature isotherms based on dye experiment for $Q = 56,100$ cfs

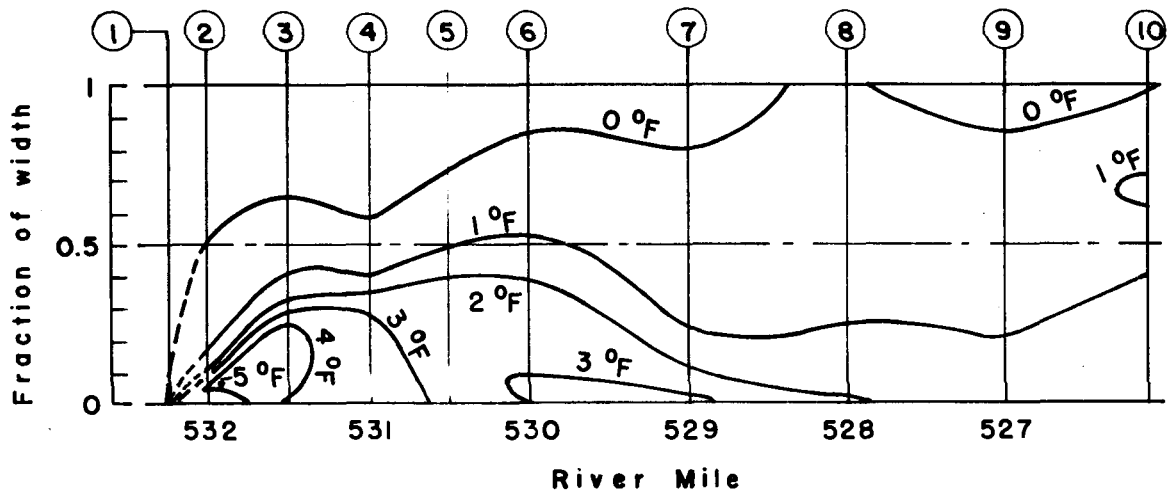
Fig. 7 indicates quite rapid initial mixing. The approximate areas enclosed by the 3.0°F, 2.5°F, 2.0°F, and 1.5°F excess-temperature isotherms are respectively 3, 11, 25, and 82 acres. By interpolation on a log-log graph, the isotherm enclosing an area of 45 acres would have an excess temperature of 1.75°F, which is well below the 5°F limit.

For lower river discharges, however, the projection is not as optimistic. Transverse mixing theory for straight uniform channels predicts that plume width at a given distance downstream from a point source is proportional to $\left(\frac{du_*}{\bar{U}}\right)^{\frac{1}{2}}$, where d = depth, \bar{U} = mean velocity of flow and u_* = shear velocity. This factor decreases, although not very strongly, with decreasing river discharge. Still, this means that for a given plant load, the excess temperature at a given point in the river would be somewhat more than doubled if the river discharge were reduced by 50 percent. The experimental results obtained by Chang (1971) in a sinuous laboratory flume, suggest that the plume width is more nearly independent of river discharge. Assuming complete independence, the excess temperature rise would be exactly inversely proportional to river discharge; i.e., to the amount of dilution water available. The isotherm pattern in Fig. 8a for a river discharge of 35,000 cfs was constructed assuming the latter, more optimistic hypothesis. At this discharge, the isotherm enclosing a 45-acre area would have an excess temperature of about 2.8°F, which is still comfortably within the limit. The results of the dye experiment therefore lead to the conclusion that the present discharge-canal arrangement should meet the proposed temperature standards during the navigation season when the river discharge is maintained at or above 30,000 cfs, provided that the ambient temperature in the river does not go above about 87°F.

The excess-temperature isotherm pattern predicted by AEC Battelle NW (1972) for the reference design case at a river discharge of 35,000 cfs is shown in Fig. 8b for comparison. The dye experiment indicates more rapid initial mixing and also a significant inward displacement of the 2°F isotherm.

Extending the results on Fig. 7 to still lower river discharges, it would appear that the area enclosed by the 5°F excess-temperature isotherm would begin to exceed 45 acres at a river discharge of about 20,000 cfs. Consequently it is concluded that some form of supplemental mixing scheme,

a. Prediction based on dye experiment



b. AEC Battelle NW prediction (Reference Design)

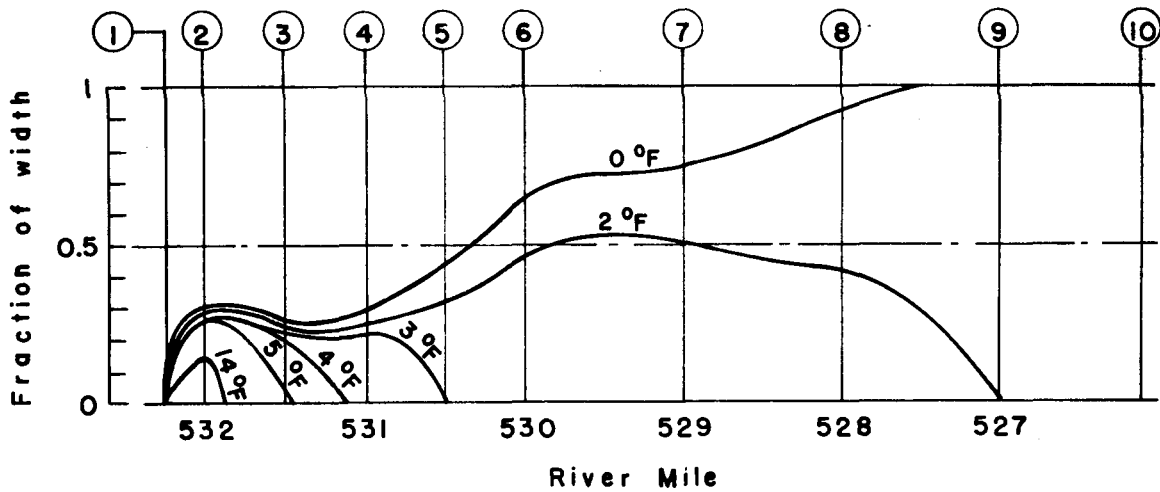


Fig. 8.— Comparison between excess temperature isotherms based on dye experiment, and isotherms predicted by AEC Battelle NW for reference design, at $Q = 35,000$ cfs

capable of achieving a dilution factor of $18/5 = 3.6$ within an area of 45 acres will be required in order to meet the proposed standards during the winter months. However, considering that the river flow is concentrated toward the Nebraska side, this should be achievable with a fairly simple single-point discharge structure, oriented at right angles to the river flow. The increased velocity in the present discharge canal, which will occur at lower river stages, will not be sufficient to produce the required mixing.

VI. NUMERICAL SIMULATION OF TRANSVERSE MIXING PROCESS

A. Mathematical Model. Mathematical models based on the classical Fickian diffusion equation predict transverse concentration distributions quite well for reasonably straight and uniform channels wherein the velocity is more or less constant across the width. However in a channel such as the Missouri River this ideal combination of circumstances does not exist and the classical model cannot be expected to provide more than a crude representation of the overall transverse mixing process.

To predict transverse concentration distributions in rivers more accurately, factors such as the variation in depth and velocity across and along the channel, varying width, and secondary flow, have to be taken into account. For this study a simulation model was adopted, similar to the one employed by Yotsukura *et al* (1970) for simulating transverse mixing in the reach of the Missouri River downstream from Blair, Nebraska.

The model is based on the steady-state convection-diffusion equation in a meandering coordinate system after Chang (1971),

$$\begin{aligned} \frac{1}{h_1} \frac{\partial}{\partial x} (uC) + \frac{\partial}{\partial y} (vC) + \frac{1}{h_1} \frac{\partial}{\partial z} (h_1 wC) \\ = \frac{1}{h_1} \frac{\partial}{\partial x} \left(\frac{\epsilon_x}{h_1} \frac{\partial C}{\partial x} \right) + \frac{\partial}{\partial y} \left(\epsilon_y \frac{\partial C}{\partial y} \right) + \frac{1}{h_1} \frac{\partial}{\partial z} \left(h_1 \epsilon_z \frac{\partial C}{\partial z} \right) \end{aligned} \quad (4)$$

wherein C = concentration; x = distance along channel axis; y = vertical distance below water surface; z = transverse distance; u , v , w = local time-averaged velocities in x , y and z directions respectively; ϵ_x , ϵ_y ,

ϵ_z = local turbulent mass transfer coefficients in x, y and z directions respectively; and h_1 = metric coefficient for meandering coordinate system which corrects longitudinal distance for curvature in channel alignment.

Using velocity distribution and cross-sectional geometry data obtained at several cross sections along the reach, the stream channel is decomposed transversely into n stream tubes of constant and equal discharge. Average velocities and cross-sectional dimensions are assigned to each stream tube at specified longitudinal intervals by means of linear interpolation between control sections wherein the transverse variations of velocity and depth have been determined by measurement. Following Chang (1971), Eq. 4 and the continuity equation for incompressible flow are integrated over the cross-sectional area of the j'th stream tube, $j = 1, 2, \dots, n$, and combined. After introducing the boundary conditions of no mass transfer across the wetted perimeter or water surface, and zero velocity at the bed, and discarding terms judged to be negligible, the system of equations reduces to

$$q_s \frac{\partial C_j}{\partial x} = \left\{ -[h_1 d \overline{w'c'^d}]_{z,x} + [h_1 d \epsilon_z^d \frac{\partial \overline{C}^d}{\partial z}]_{z,x} \right\}_{z_{j-1}}^{z_j} \quad (5)$$

In Eq. 5, $q_s = Q_R/n$ = discharge in stream tube; C_j = average concentration in j'th stream tube; the overbars followed by the superscript d represent averaging over the depth of flow, and the primed quantities deviations from this average; and z_j denotes the boundary between the j+1 'st and j'th stream tubes. If the dye tracer is fairly well distributed over the depth of flow and it is assumed by analogy with longitudinal dispersion theory that the secondary flow convection term can be represented as a transverse convective dispersion term according to the equation

$$\overline{w'c'^d} = -\epsilon_c \frac{\partial \overline{C}^d}{\partial z}, \quad (6)$$

then the two terms on the right side of Eq. 5 can be combined into a single gradient-type diffusion term with the overall transverse mixing coefficient $E_z = \epsilon_c + \epsilon_z^d$.

Eq. 5 can then be put into the finite difference form

$$C_{i+1,j} = C_{i,j} + \frac{\Delta x_i}{q_s} \left[\left(\frac{h_1 d E_z}{\Delta z} \right)_{i,j} (C_{i,j+1} - C_{i,j}) - \left(\frac{h_1 d E_z}{\Delta z} \right)_{i,j-1} (C_{i,j} - C_{i,j-1}) \right] \quad (7)$$

where i indicates the number of longitudinal distance steps of length Δx downstream from a control section; h_1 , d and E_z are all evaluated at the boundary between neighboring stream tubes; and Δz = distance between centroids of neighboring stream tubes. The metric coefficient $h_{1i,j}$, which corrects for variation in longitudinal distance along the different stream tube boundaries due to channel curvature, is calculated by the approximate equation

$$h_{1i,j} = \frac{L_R}{L} + \frac{(L_L - L_R)}{L} \left\{ \left(\frac{z_j}{W} \right)_k + \left[\left(\frac{z_j}{W} \right)_{k+1} - \left(\frac{z_j}{W} \right)_k \right] \left(\frac{i \Delta x}{L} \right) \right\} \quad (8)$$

wherein L , L_R and L_L = longitudinal distances between the k 'th and $k+1$ 'st control sections measured along the channel centerline, right bank, and left bank, respectively; $(z_j/W)_k$ = fractional distance across channel from the right bank to the boundary between the $j+1$ 'st and j 'th stream tubes at the k 'th control section; and i = number of steps of length Δx downstream from the k 'th control section.

The boundary condition corresponding to the requirement of no mass transfer across the channel boundaries is that no exchange is permitted across the outer boundaries of the outermost stream tubes. It can be stated mathematically as

$$\left(\frac{h_1 d E_z}{\Delta z} \right)_{i,j} (C_{i,j+1} - C_{i,j}) = 0 \quad (9)$$

for $j=0$ and $j=n$.

B. Representation of the River as a Set of Stream Tubes. The river channel was divided into 20 imaginary stream tubes, each carrying the same discharge, and numbered from right to left, according to the scheme shown in Fig. 9. The stream tubes are not bounded by streamlines in the

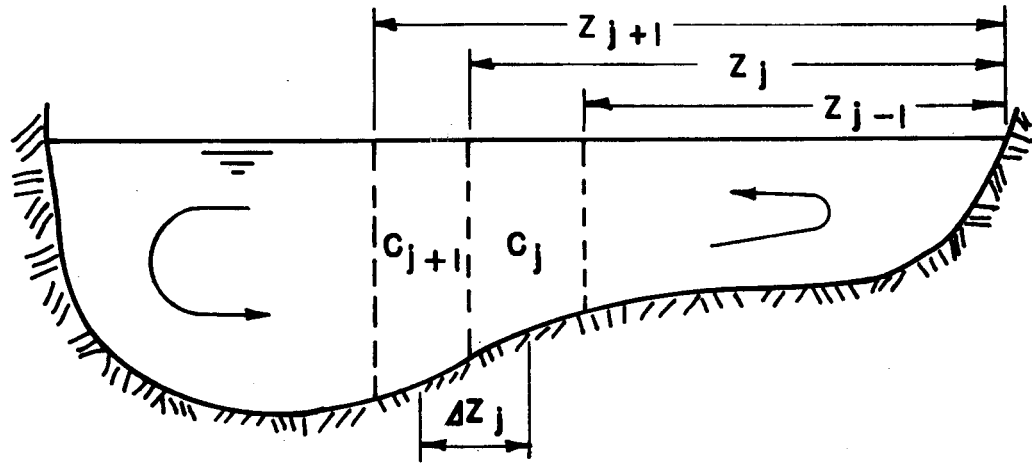


Fig. 9.—Definition sketch for stream tubes

usual sense, but by imaginary vertical walls. According to this definition, there is no net flow across stream tube boundaries, however, there is mass transfer between adjacent stream tubes due to both turbulent diffusion and convection by secondary flow.

Transects 2-10, where dye samples were obtained, were used as the control sections. The velocity distribution and cross-sectional geometry data from the U.S. Geological Survey measurements were directly applicable for Transects 3, 5, 7 and 10. For the remaining transects, the cross-sectional geometry data were obtained from depth soundings reported in the Corps of Engineers Missouri River Hydrographic Survey (1967), and the transverse distribution of the normalized discharge per unit width q/\bar{q} was synthesized from q/\bar{q} distributions for cross sections having similar shapes. This was done with the aid of q/\bar{q} vs d/\bar{d} plots such as Fig. 10, which is based on data from the cross sections at Miles 531.5, 530.5, and 527.5. The q/\bar{q} distributions for Transects 4 and 6 were synthesized using data from Miles 531.5 and 530.5, and the distributions for Transects 2, 8 and 9 with data from Mile 527.5.

Note that the data points on Fig. 10 fall fairly close to the relationship

$$\frac{q}{\bar{q}} = \left(\frac{d}{\bar{d}}\right)^{5/3} \quad (10)$$

based on the Manning formula. The senior writer has tested this relationship with transverse flow distribution data from the Mississippi and Illinois Rivers as well, and found it to be fairly reliable.

The stream tube boundaries at each control section were determined by reading the z values corresponding to each incremental increase of 0.05 from a plot of the cumulative normalized discharge, q_c/Q_R vs z . The vertical and horizontal dimensions of a stream tube are assumed to vary linearly between successive control sections. This specifies its cross-sectional area at any longitudinal position between control sections, which in turn, together with continuity, specifies the average velocity in the stream tube. Actually, Eq. 7 is set up so as to require only the depth at each stream tube boundary and the transverse distance between the centroids of adjacent stream tubes at longitudinal intervals of $h_1 \Delta x$.

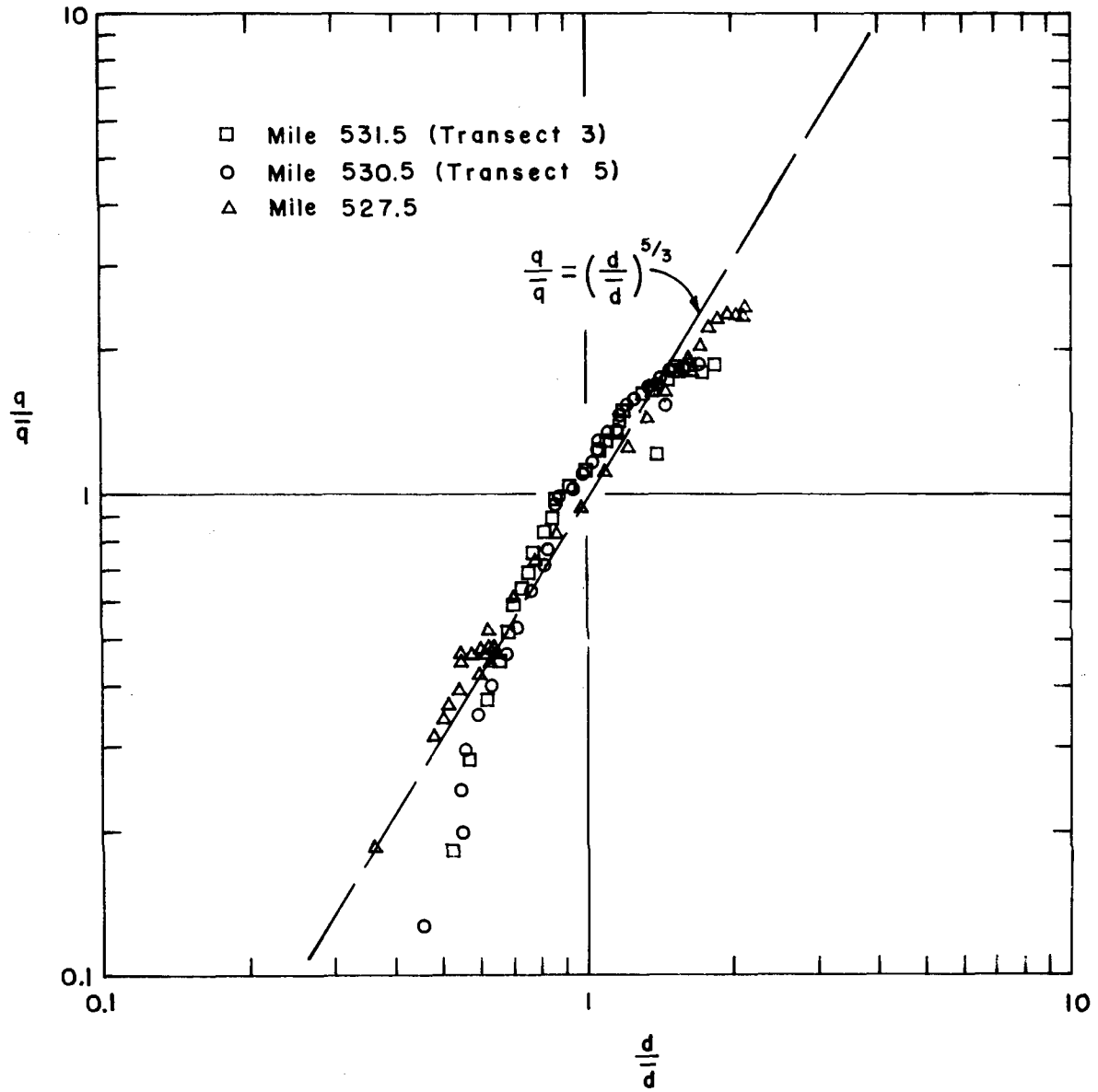


Fig. 10.—Relative unit discharge versus relative depth relationship for synthesizing transverse distribution of unit discharge

C. Determination of Concentration Distribution and Transverse Mixing Coefficients by the Simulation Method. The simulation method of representing the mixing process involves a step-by-step numerical solution of Eq. 7. This was carried out on the IBM 360/65 Computer at The University of Iowa Computer Center. The background data required by the program includes the river discharge, the stream tube dimensions at each control section, the longitudinal distances between control sections measured along the channel centerline and both banks, and the transverse mixing coefficient, E_z . The transverse concentration distribution at the upstream control section is read in as the initial condition. Then for each succeeding longitudinal distance step of length $h_1 \Delta x$, Eq. 7 is solved successively for the concentration in each stream tube, using the concentrations computed in the previous step. The required stream-tube dimensions are computed at each step from the control-section data according to the rules outlined in the previous section.

Selection of mesh size is a critical consideration in the numerical solution of finite difference equations. For explicit forward difference schemes such as Eq. 7, a useful stability criterion is that the value of the multiplier, $h_1 dE_z \Delta x / q_s \Delta z$, of the difference terms, not be permitted to exceed $1/2$. All of the terms in the multiplier except E_z and Δx are fixed by the stream-tube geometry. So, in conformance with the criterion, a step length of $\Delta x = 50$ ft was used for $E_z < 42$ ft²/sec, and a step length of $\Delta x = 15$ ft was used for $E_z > 42$ ft²/sec. If there was any indication of instability in the results, Δx was reduced. Also when the results appeared to be satisfactory, the computer run was repeated using a smaller value of Δx as a check. For most of the computer runs, $\Delta x = 50$ ft was found to be adequate.

The best value of E_z to use in the subreach, between two successive control sections was determined by a trial and error, least-squares procedure. Using the normalized transverse concentration distribution, based on experimental data, as the initial distribution at the upstream control section, the transverse concentration distribution at the downstream control section was computed using the simulation model. This procedure was repeated for several different values of E_z . The best value of E_z was taken to be the one which gave the best least-squares fit between the computed distribution and

the normalized distribution, based on experimental data, at the downstream control section. The values of E_z , determined in this manner for each subreach, are shown in Fig. 11.

Having determined the appropriate E_z values, the concentration distribution along the entire test reach downstream from Transect 2 was then computed by the simulation model using the normalized observed distribution for Transect 2 as the input distribution. This was done using the different E_z values for the different subreaches that are shown in Fig. 11, and also using a constant E_z value of $11.94 \text{ ft}^2/\text{sec}$ which is fairly representative for most of the test reach. The results for Transects 3-10 are shown in Figs. 12a-12c, wherein the results for both sets of computations are compared with the normalized distributions based on experimental data. As expected, the computed distributions based on the variable E_z match the experimental distributions more closely. However, there is little difference between the computed distributions at Transect 10, because the cumulative effects of the variable E_z tends to average out over the entire length of the test reach.

VII. THE TRANSVERSE MIXING COEFFICIENT

A. As Determined by Simulation Method. The variation of E_z along the channel as determined by the simulation method, is shown in Fig. 11. The value of E_z attains maximum values in the subreaches between Transects 5 and 6 and between Transects 9 and 10, and attains minimum values in the subreaches between Transects 2 and 3 and between Transects 6 and 7. Reference to Fig. 2 shows that the two maxima occur toward the downstream ends of the two bends, and that the minima occur at about the beginning of the first bend and in the relatively straight reach between the first and second bends. This is consistent with the results obtained in Chang's (1971) laboratory flume experiments wherein the maximum E_z values occurred most frequently in the downstream part of bends, but occasionally near the middle, and the minimum values occurred most frequently in the upstream part of bends, but occasionally near the downstream end of the straight reach between bends. Chang concluded that the pattern of longitudinal variation of E_z is closely related to the growth-decay-reversal cycle of the bend-generated secondary flow, with the

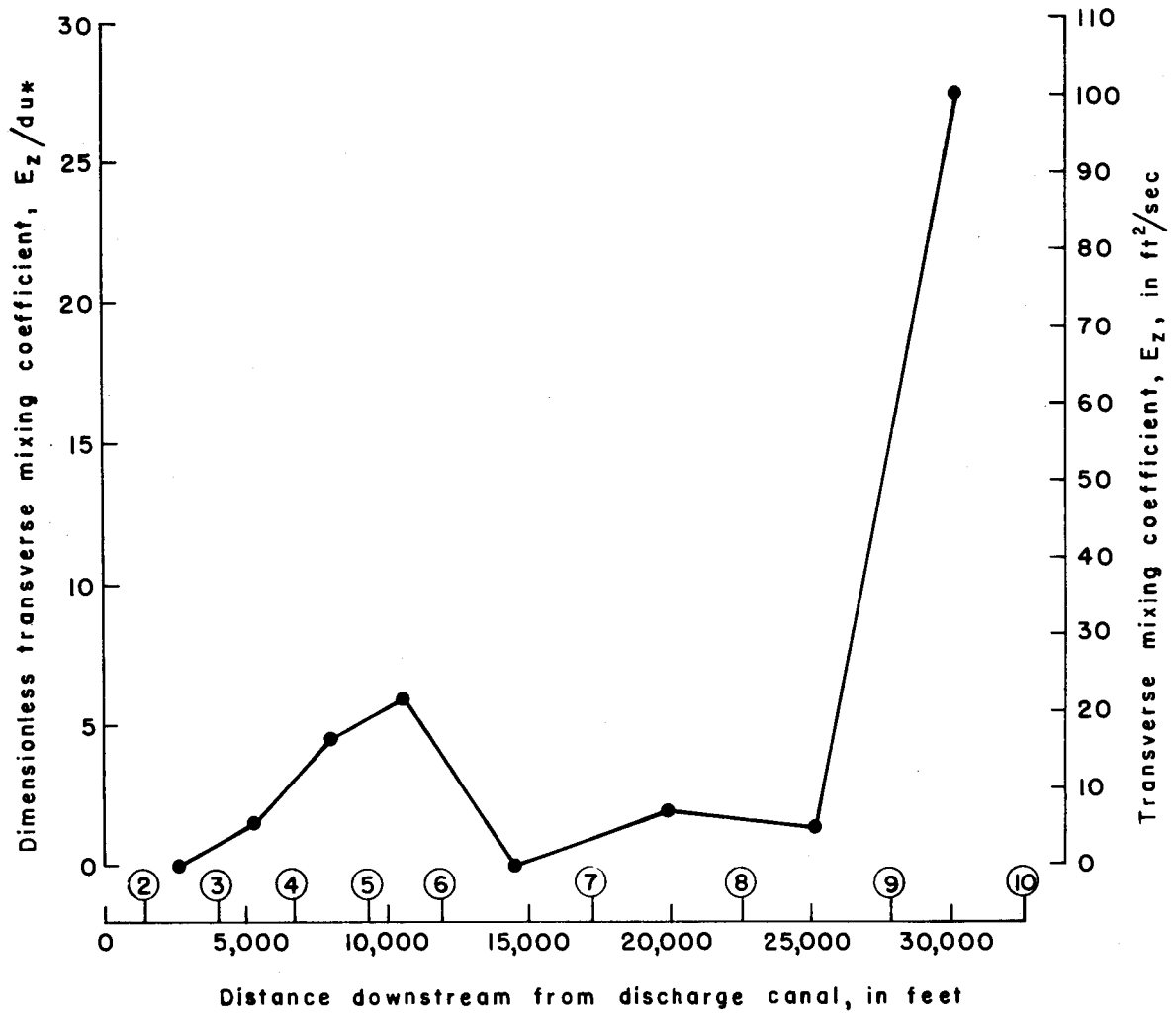


Fig. 11.—Variation of transverse mixing coefficient along test reach as determined by simulation method

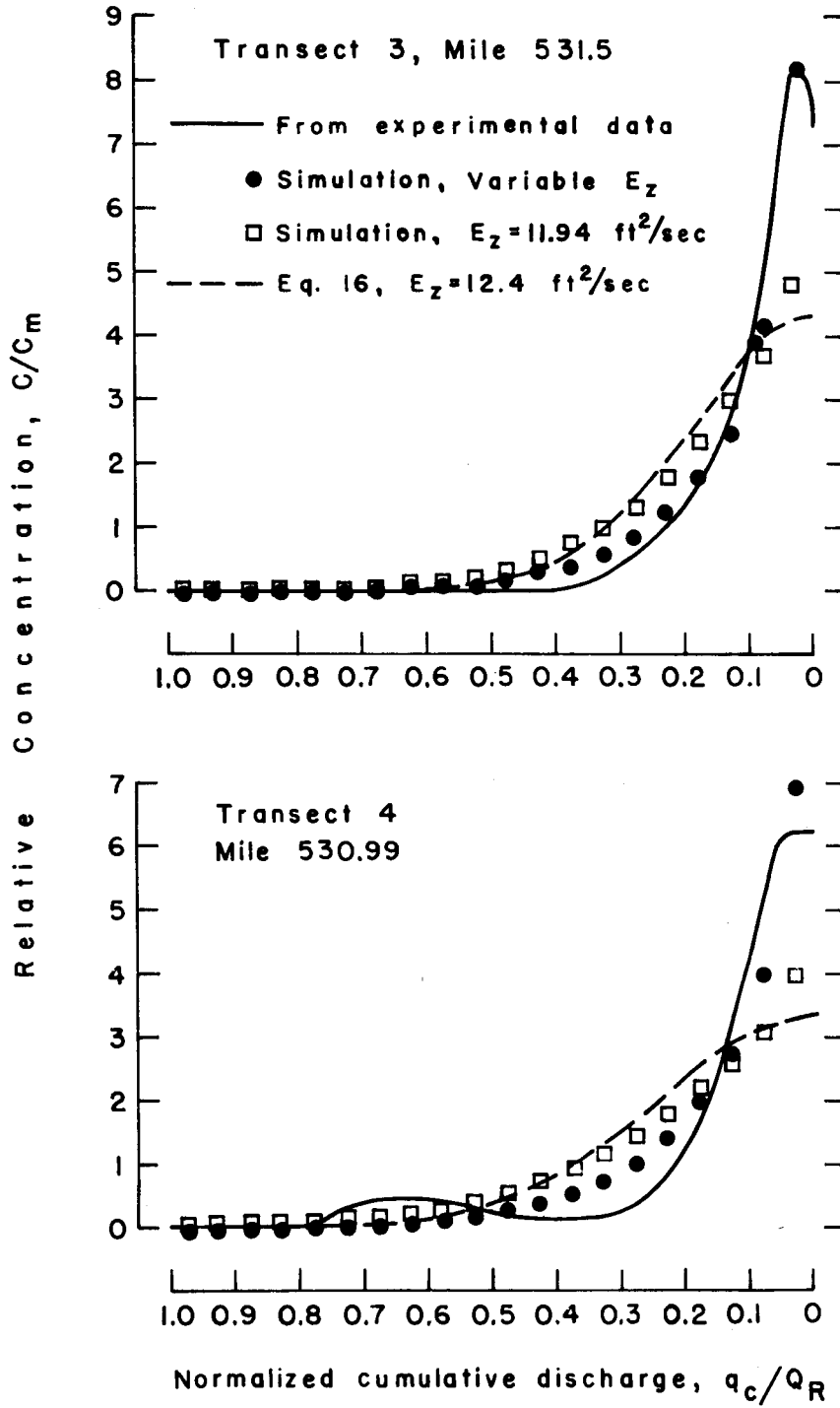


Fig. 12 a.— Comparison between simulated and measured transverse concentration distributions, Transects 3 and 4

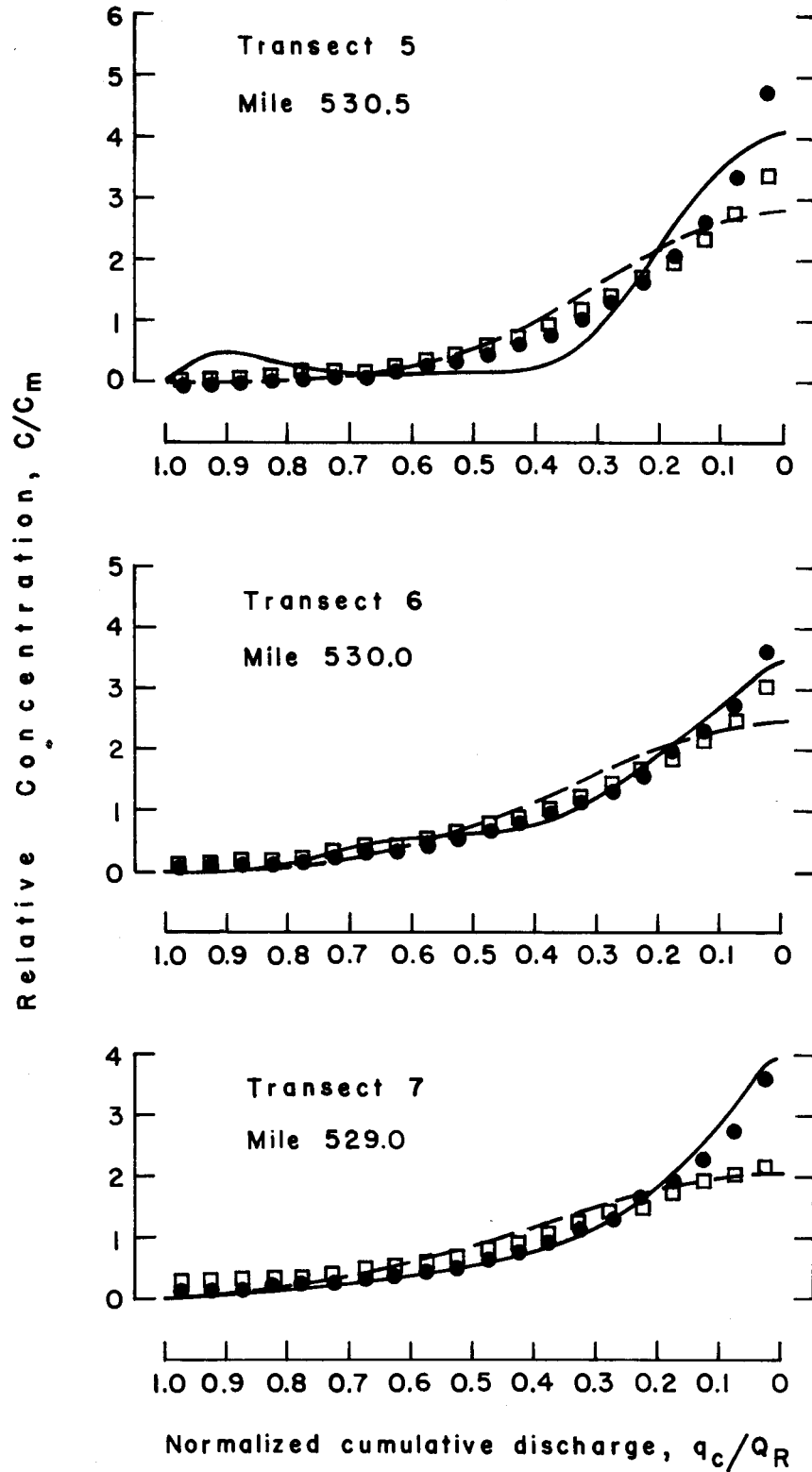


Fig. 12 b.— Comparison between simulated and measured transverse concentration distributions, Transects 5, 6 and 7

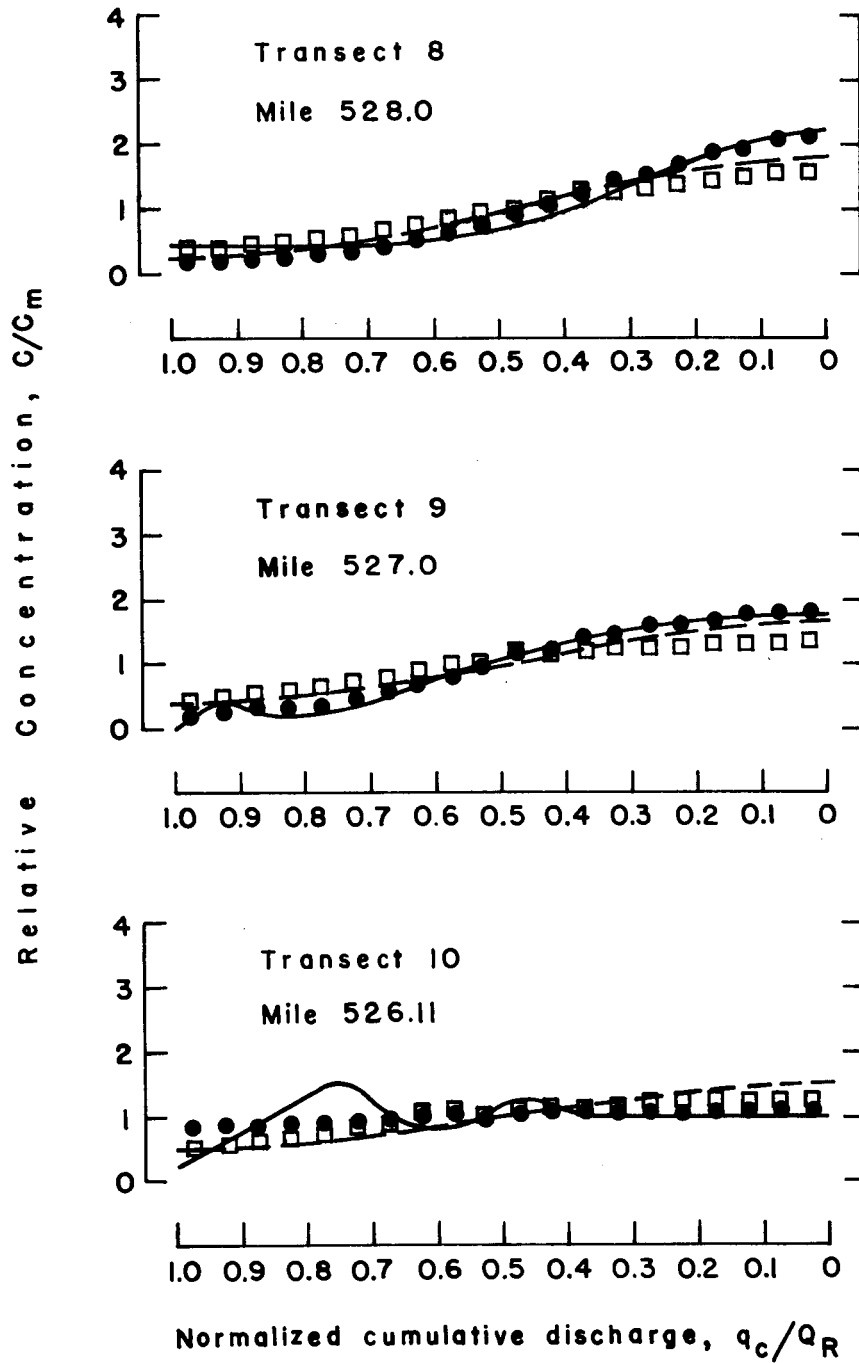


Fig. 12 c.— Comparison between simulated and measured transverse concentration distributions, Transects 8, 9 and 10

maximum values occurring where the secondary flow reaches maximum development, and minimum values occurring in the region where reversal occurs. In Fig. 11 the maximum value of E_z in the second bend is nearly five times that observed in the first bend, but then the second bend is much sharper which would give rise to more intense transverse convective transport due to secondary flow.

The values of the dimensionless transverse mixing coefficient E_z/du_* were computed using the overall average depth of $d = 13$ ft and shear velocity of $u_* = \sqrt{gdS} = 0.28$ ft/sec. The maximum E_z/du_* values considerably exceed the maximum values of 2 to 3 typically observed in Chang's experiments, and the estimated maximum value of 1.2 for the Missouri River reach downstream from Blair, Nebraska, Yotsukura *et al* (1970). The maximum E_z/du_* values for the two bends and the one for the Blair reach are approximately proportional to the square of the depth to radius of curvature ratio. This is in accord with Fischer's (1969) prediction, based on Rozovskii's (1957) radial velocity distribution function for an idealized curved channel, according to which

$$\frac{E_z}{du_*} \approx \left(\frac{\bar{U}}{u_*}\right)^2 \left(\frac{d}{r_c}\right)^2. \quad (11)$$

The approximate radii of curvature for the three bends in question are 6,400 ft and 3,400 ft for the Langdon and Aspinwall bends in the reach downstream from the Cooper Station, and 12,000 ft for the bend downstream from Blair. The average depth in the Blair reach at the time of that experiment was about 9 ft. The values of \bar{U}/u_* were very nearly the same for both reaches.

So far as the writers know, the maximum E_z/du_* values reported here for the reach downstream from the Cooper Nuclear Station are larger than any previously published values.

B. As Determined by the Method of Moments. For the reasons indicated in Section IV-C, the method of moments as applied by Yotsukura and Cobb (1972) to the distribution of C with respect to the cumulative discharge q_c , as in Figs. 6a-6d, is much better suited to sinuous, non-uniform channels such as the Missouri River than is the method of moments

as applied by Yotsukura *et al* (1970) to the distribution of C with respect to the transverse position z, as in Figs. 5a-5d. Therefore only the former application is considered here.

Yotsukura and Cobb, by introducing the cumulative discharge

$$q_c = \int_0^z q dz = \int_0^z \bar{U}^d d dz \quad (12)$$

as a new variable, showed that the steady state convection-diffusion equation, averaged over the depth, could be transformed to the equation

$$\frac{\partial C}{\partial x} = \frac{\partial}{\partial q_c} \left(E_z \bar{U}^d d^2 \frac{\partial C}{\partial q_c} \right). \quad (13)$$

If, for simplicity, the product $E_z \bar{U}^d d^2$ is treated as a constant "diffusion" factor, say D, then Eq. 13 assumes the same form,

$$\frac{\partial C}{\partial x} = D \frac{\partial^2 C}{\partial q_c^2} \quad (13a)$$

as the classical Fickian diffusion equation for which solutions corresponding to many initial conditions are well known. In accordance with Fickian diffusion theory, the diffusion factor can be determined from experimental C vs q_c/Q_R curves like those in Figs 6a-6d by means of the relationship

$$D = \frac{1}{2} \frac{d\sigma_{q_c}^2}{dx} \quad (14)$$

where $\sigma_{q_c}^2$ is the variance (second moment about the mean) of the distribution of C with respect to q_c . The variance in this case, where the source is located at one bank which is assumed to behave as a reflecting barrier, is defined by the equation

$$\sigma_{q_c}^2 = \frac{\int_0^Q q_c^2 C dq_c}{\int_0^Q C dq_c} \quad (15)$$

Eq. 14 is valid only until the tracer plume encounters the bank opposite from the source. In this case the dye plume barely touches the Missouri

shore, so Eq. 14 should be applicable over virtually the entire test reach. The variance $\sigma_{q_c}^2$ is shown as a function of x in Fig. 13. The value of the "diffusion" factor D , according to Eq. 14 and the line drawn through the data points, is $13,600 \text{ (cfs)}^2/\text{ft}$. Putting in the overall average depth $\bar{d} = 13 \text{ ft}$, and velocity $\bar{U} = 6.5 \text{ ft/sec.}$, and solving for E_z , gives $E_z = 12.4 \text{ ft}^2/\text{sec}$, which is close to the representative constant value used in the simulation method.

For comparison, the solution of Eq. 13a, for the initial condition of a vertical line source at the end of the discharge canal is shown on Figs. 12a-12c together with the results obtained by the simulation method. The mathematical form of the solution is the Gaussian function

$$\frac{C}{C_m} = \frac{Q_R}{\sqrt{\pi D x}} \exp \left[- \frac{(q_c/Q_R)^2}{4 D x / Q_R^2} \right]. \quad (16)$$

Eq. 16 and the simulation results for the case of the constant E_z tend to converge with increasing x , as the effects of variations in d and \bar{U}^d , which are not accounted for in Eq. 16, are averaged out.

Essentially the same kind and amount of velocity distribution and channel geometry data is required for both the simulation and moment methods. The method of moments has the advantage of computational simplicity, but the simulation method is more responsive to the variation of conditions in the longitudinal direction. The finite difference form of Eq. 13, if the product $E_z \bar{U}^d d^2$ is not treated as a constant and the three components are permitted to vary individually, is essentially identical to Eq. 7, the stream tube equation, that was used in the simulation method, so there is no fundamental difference between the Yotsukura-Cobb and stream tube representations of the transverse mixing process. Overall, the writers prefer the simulation method for prediction purposes. However in investigations such as the present one, the method of moments is useful for obtaining trial values of E_z to use in the simulation method.

VIII SUMMARY AND CONCLUSIONS

Rhodamine WT dye was used as a tracer to experimentally simulate the waste heat in the condenser cooling water which will be discharged into

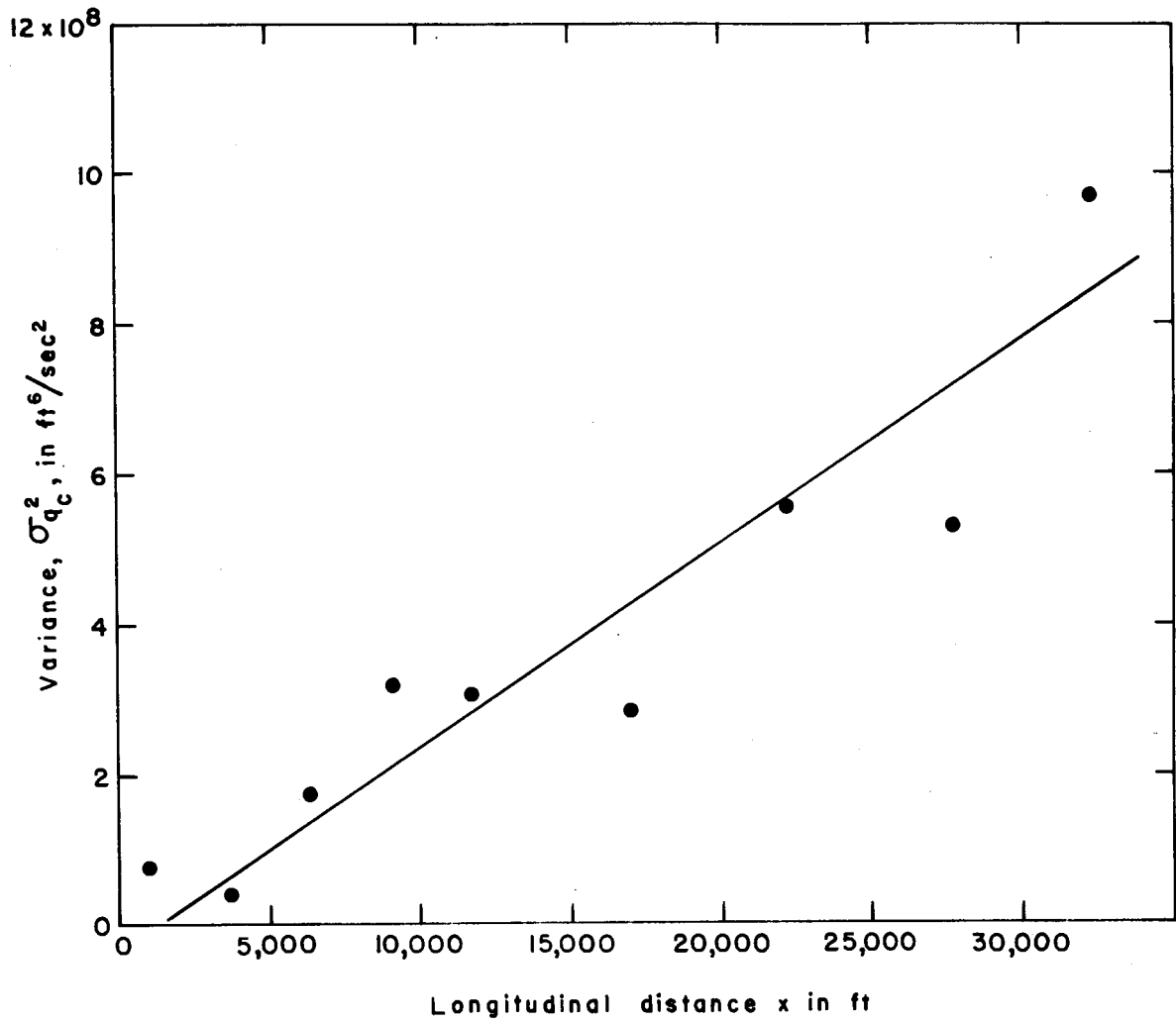


Fig. 13.—Variance, $\sigma_{q_c}^2$, as a function of longitudinal distance

the Missouri River from the Cooper Nuclear Station after it goes into operation. The dye was introduced continuously into the once-through cooling system, where it mixed with the circulating water before entering the river through the plant discharge canal. Transverse profiles of dye concentration, velocity, and depth were experimentally determined at several cross sections in the six-mile reach downstream from the plant, which contains two bends, one of which is very sharp.

Based on the results of the experiment it is estimated that the isotherm enclosing a 45-acre mixing zone would have an excess temperature of 1.75°F which is well below the 5°F limit which would be allowed by the proposed temperature standards. However, the river discharge at the time of the experiment was 56,100 cfs, which considerably exceeds the typical navigation-season flows of about 35,000 cfs, and the wintertime low flows which are frequently less than 10,000 cfs. Extending the experimental results to lower river discharges, it is estimated that the 5°F limit at the perimeter of a 45-acre mixing zone would be exceeded when the river discharge decreases to less than about 20,000 cfs. This indicates that some sort of supplemental mixing scheme capable of achieving a dilution factor of 3.6 within a 45-acre mixing zone will be required in order to meet the proposed temperature standards during the winter months.

A more detailed analysis of the experimental data indicated that an overall representative value of the transverse mixing coefficient for most of the test reach is about 12 ft²/sec, corresponding to a value of the dimensionless mixing coefficient of $E_z/du_* = 3.3$. Values of E_z/du_* ranging from zero to about 27 were found in different sections along the reach. The representative and maximum values, so far as the writers know, are higher than any previously published values. The pattern of variation of E_z/du_* with respect to position along the bends is consistent with results obtained in previous experiments in a sinuous laboratory flume.

A mathematical model based on the steady state convection-diffusion equation was used to simulate the transverse mixing process. When the experimentally-determined cross-sectional geometry, velocity distribution data, and transverse mixing coefficients are put into the model, it predicts transverse concentration distribution profiles that agree quite well with the measured profiles.

REFERENCES

1. Chang, Y.C., "Lateral Mixing in Meandering Channels", thesis presented to The University of Iowa, at Iowa City, Iowa, in 1971, in partial fulfillment of the requirements for the degree of Doctor of Philosophy, 195 pp.
2. Fischer, H.B., "The Effect of Bends on Dispersion in Streams", *Water Resources Research*, Vol. 5, No. 2, April 1969, pp. 496-506.
3. Prych, E.A., "Effects of Density Differences on Lateral Mixing in Open-Channel Flows", *Report No. KH-R-72*, California Institute of Technology, 1970, 225 pp.
4. Rozovskii, I.L., "Flow of Water in Bends of Open Channels", *Academy of Sciences of the Ukrainian Soviet Socialist Republic*, 1957, (translation No. OTS60-51133, Office of Technical Services, U.S. Dept. of Commerce, Washington, D.C.)
5. Ryan, P.J., and Stolzenbach, K.D., "Environmental Heat Transfer", Chapter 1 of Volume I, *Engineering Aspects of Heat Disposal from Power Generation*, Lecture Notes for Special Summer Program 1.765, R.M. Parsons Lab for Water Resources and Hydrodynamics, Massachusetts Institute of Technology, 1972, pp. 1-1-1-75.
6. U.S. Army Engineer District, Omaha, "Missouri River Hydrographic Survey, Omaha District, Ponca to Rulo," Corps of Engineers, Omaha, Nebraska, 1967.
7. U.S. Atomic Energy Commission, Battelle NW, "Staff Analysis of Alternate Heat Dispersion from the Cooper Nuclear Station."
8. Yotsukura, N., and Cobb, E.D., "Transverse Diffusion of Solutes in Natural Streams," *U.S. Geological Survey Professional Paper 582-C*, 1972, 19 pp.
9. Yotsukura, N., Fischer, H.B., and Sayre, W.W., "Measurement of Mixing Characteristics of the Missouri River between Sioux City, Iowa, and Plattsmouth, Nebraska," *U.S. Geological Survey Water Supply Paper 1899-G*, 1970, 29 pp.